Manuscript Details

Manuscript number	COMPAG_2017_626
Title	Development of a single energy balance model for prediction of temperatures inside a naturally ventilated greenhouse with polypropylene soil mulch
Article type	Research Paper

Abstract

In this study, a semi-empirical dynamic model of energy balance was developed to predict temperatures (air, plants, greenhouse cover and soil) in a naturally ventilated greenhouse with a polypropylene mulch covering the soil in a Mediterranean climate. The model was validated using experimental data of 5 non-successive periods of 5 days throughout the crop season in the province of Almería (Spain). During the evaluation period, the transmissivity of the cover ranged between 0.44 and 0.80 depending on whitening, and the leaf area index of the tomato crops growing inside the greenhouse varied from LAI=0.74 to 1.30 m2 m–2. The model mainly consists of a system of 6 non-linear differential equations of energy conservation at inside air, greenhouse plastic cover, polypropylene mulch and three layers of soil. We used multiple linear regressions to estimate the crop temperature in a simple way that allows a reduction in the number of parameters required as input. The main components of the energy balance in warm climate conditions are the solar radiation, the heat exchanged by natural ventilation and the heat stored in the soil. To improve the estimation of the heat exchanged by ventilation, different discharge coefficients were used for roof CdVR and side openings CdVS. Both coefficients changed throughout the time as a function of the height and opening angle of the windows and of the air velocity across the insect-proof screens. The model also used different wind effect coefficients Cw for Northeast or Southwest winds, to take into account the different obstacles (a neighbouring greenhouse at the south and a warehouse at the north). A linear regression of the wind direction angle θw was used as correction function for the volumetric ventilation flux G. The results showed that the accuracy of the model is affected mainly by errors in the cover transmissivity on cloudy days (when diffuse radiation prevails) and errors in the temperature of air exiting the greenhouse on windy days (when hot air stagnated near roof openings, that were closed by the climate controller to avoid wind damage). In general, the results of validation comparing calculated values with those measured on 25 days (with relative root mean square errors below 10%), show sufficient accuracy for the model to be used to estimate air, crop, plastic cover, polypropylene mulch and soil temperatures inside the greenhouse, and as a design tool to optimise the ventilation system characteristics and control settings.

Keywords	Greenhouse; dynamic model; natural ventilation; thermal analysis; plastic mulch

Corresponding Author	Francisco Domingo Molina-Aiz
Corresponding Author's Institution	Unversidad de Almería
Order of Authors	Audberto Reyes-Rosas, Francisco Domingo Molina-Aiz, Diego Luis Valera Martinez, Alejandro López, Sasirot Khamkure
Suggested reviewers	Emmanuel Mashonjowa, Ahmed Abdel-Ghany, Fatima Baptista, Hicham Fatnassi

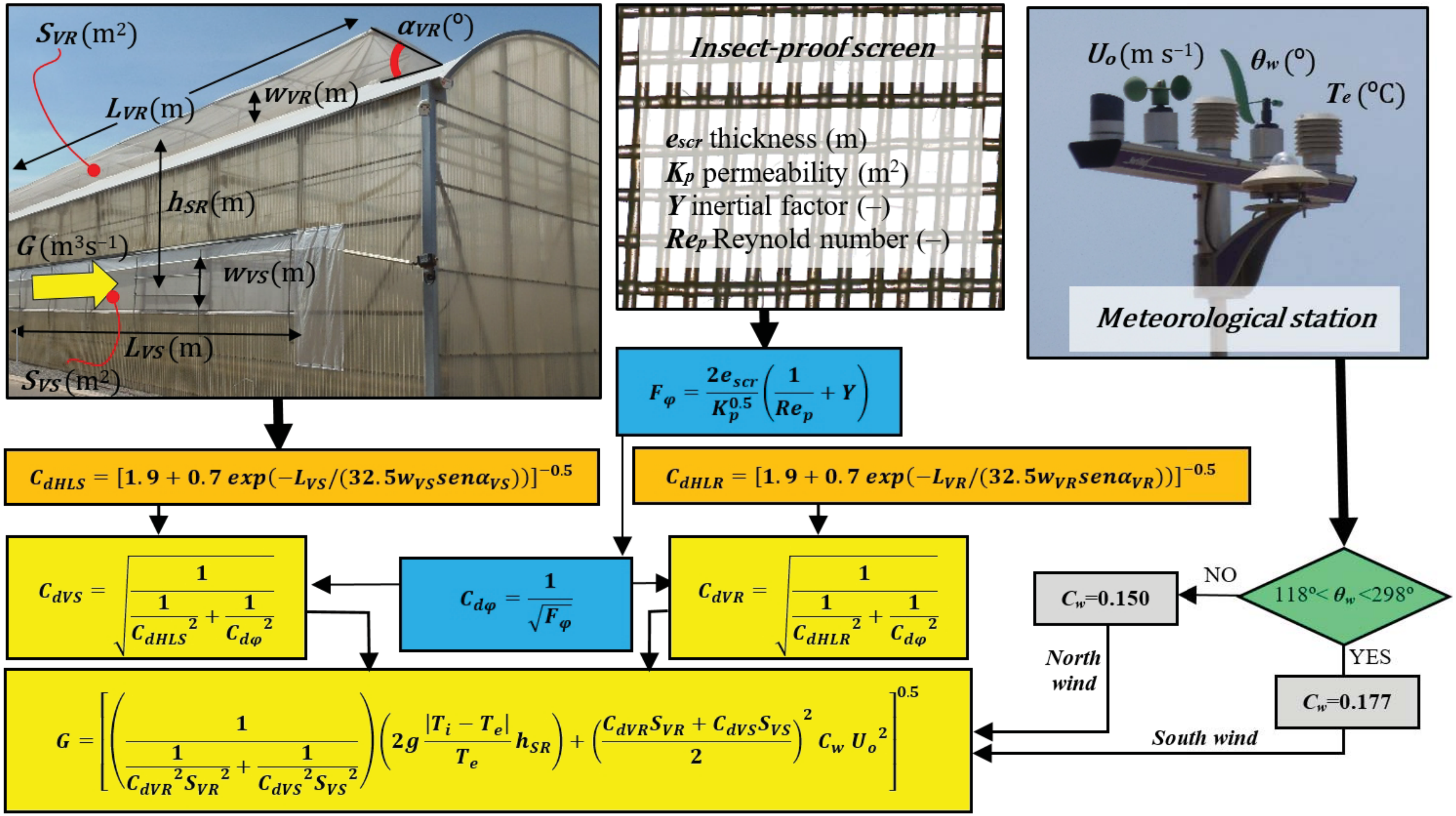

S_{VR} (m²)
α_{VR} (°)
L_{VR} (m)
w_{VR} (m)
h_{SR} (m)
G (m³s⁻¹)
w_{VS} (m)
L_{VS} (m)
S_{VS} (m²)
Insect-proof screen
e_{scr} thickness (m)
K_p permeability (m²)
Y inertial factor (–)
Re_p Reynold number (–)
U_o (m s⁻¹)
θ_w (°)
T_e (°C)
Meteorological station
$F_\varphi = \frac{2e_{scr}}{K_p^{0.5}}\left(\frac{1}{Re_p} + Y\right)$
$C_{dHLS} = [1.9 + 0.7\,exp(-L_{VS}/(32.5 w_{VS} sen\alpha_{VS}))]^{-0.5}$
$C_{dHLR} = [1.9 + 0.7\,exp(-L_{VR}/(32.5 w_{VR} sen\alpha_{VR}))]^{-0.5}$
$C_{dVS} = \sqrt{\frac{1}{\frac{1}{C_{dHLS}^2} + \frac{1}{C_{d\varphi}^2}}}$
$C_{d\varphi} = \frac{1}{\sqrt{F_\varphi}}$
$C_{dVR} = \sqrt{\frac{1}{\frac{1}{C_{dHLR}^2} + \frac{1}{C_{d\varphi}^2}}}$
$118° < \theta_w < 298°$
NO
YES
C_w=0.150
C_w=0.177
North wind
South wind
$G = \left[\left(\frac{1}{\frac{1}{C_{dVR}^2 S_{VR}^2} + \frac{1}{C_{dVS}^2 S_{VS}^2}}\right)\left(2g\frac{|T_i - T_e|}{T_e}h_{SR}\right) + \left(\frac{C_{dVR}S_{VR} + C_{dVS}S_{VS}}{2}\right)^2 C_w U_o^2\right]^{0.5}$

Development of a single energy balance model for prediction of temperatures inside a naturally ventilated greenhouse with polypropylene soil mulch

Audberto Reyes-Rosas, Francisco D. Molina-Aiz*, Diego L. Valera, Alejandro López, Sasirot Khamkure

Research Centre CIAIMBITAL, University of Almería, Ctra. Sacramento s/n, 04120 Almería, Spain.

** Corresponding author. E-mail addresses: fmolina@ual.es*

Abstract

In this study, a semi-empirical dynamic model of energy balance was developed to predict temperatures (air, plants, greenhouse cover and soil) in a naturally ventilated greenhouse with a polypropylene mulch covering the soil in a Mediterranean climate. The model was validated using experimental data of 5 non-successive periods of 5 days throughout the crop season in the province of Almería (Spain). During the evaluation period, the transmissivity of the cover ranged between 0.44 and 0.80 depending on whitening, and the leaf area index of the tomato crops growing inside the greenhouse varied from L_{AI}=0.74 to 1.30 m^2 m^{-2}. The model mainly consists of a system of 6 non-linear differential equations of energy conservation at inside air, greenhouse plastic cover, polypropylene mulch and three layers of soil. We used multiple linear regressions to estimate the crop temperature in a simple way that allows a reduction in the number of parameters required as input. The main components of the energy balance in warm climate conditions are the solar radiation, the heat exchanged by natural ventilation and the heat stored in the soil. To improve the estimation of the heat exchanged by ventilation, different discharge coefficients were used for roof C_{dVR} and side openings C_{dVS}. Both coefficients changed throughout the time as a function of the height and opening angle of the windows and of the air velocity across the insect-proof screens. The model also used different wind effect coefficients C_w for Northeast or Southwest winds, to take into account the different obstacles (a neighbouring greenhouse at the south and a warehouse at the north). A linear regression of the wind direction angle θ_w was used as correction function for the volumetric ventilation flux G. The results showed that the accuracy of the model is affected mainly by errors in the cover transmissivity on cloudy days (when diffuse radiation prevails) and errors in the temperature of air exiting the greenhouse on windy days (when

hot air stagnated near roof openings, that were closed by the climate controller to avoid wind damage). In general, the results of validation comparing calculated values with those measured on 25 days (with relative root mean square errors below 10%), show sufficient accuracy for the model to be used to estimate air, crop, plastic cover, polypropylene mulch and soil temperatures inside the greenhouse, and as a design tool to optimise the ventilation system characteristics and control settings.

Keywords: Greenhouse, dynamic model, natural ventilation, thermal analysis, plastic mulch.

Nomenclature

Alphabetic symbols

C_{dVR} roof vent discharge coefficients (-)

C_{dVS} side vent discharge coefficients (-)

C_{dHLj} discharge coefficient of the unscreened openings j (-)

$C_{d\varphi}$ discharge coefficient of the insect proof screens (-)

c_{pa} specific heat of the air inside the greenhouse (J kg^{-1} K^{-1})

c_{pc} specific heat of the greenhouse cover material (J kg^{-1} K^{-1})

c_{sjk} specific heat of the soil between deeps z_j and z_k (J kg^{-1} K^{-1})

c_{spm} specific heat of the polypropylene mulch (J kg^{-1} K^{-1})

C_w wind effect coefficient (–)

D_r thread density or number of thread per centimetre in each direction (threads cm^{-1} × threads cm^{-1})

e_c cover thickness (m)

e_{sjk} soil layer thickness between depth z_j and z_k (m)

e_{scr} insect-proof screen thickness (m)

e_{spm} polypropylene mulch sheet thickness (m)

E_{xy} precision of measurement of the thickness (μm)

f_G ventilation flux correction coefficient (–)

F_φ pressure loss coefficient of the insect-proof screen (–)

g gravitational constant (m s^{-2})

G volumetric ventilation flow (m^3 s^{-1})

h_{ci} convective heat transfer coefficient between interior air and greenhouse cover (W m^{-2} K^{-1})

h_{co} outside air-cover convective coefficient (W m^{-2} K^{-1})

h_{si} inside air-cover convective coefficient (W m^{-2} K^{-1})

H_{SR} vertical distance between the midpoint of side and roof openings (m)

h_{vi} convective heat transfer coefficient between interior air and plant leaves (W m^{-2} K^{-1})

k_L extinction coefficient for conical leaves distribution (–)

K_p insect-proof screen permeability (m^2)

k_s extinction coefficient of plants for shortwave radiation (–)

k_{sjk} thermal conductivity of soil layer between depth z_j and z_k (W m^{-1} K^{-1})

L_{AI} leaf area index (m^2 m^{-2})

L_b mean path length of solar beam radiation (m)

L_{cl} characteristic leaf length (m)

L_{Vj} length of the opening j (m)

n number of measurements (–)

P_e pressure outside the greenhouse (Pa)

P_v proportion of area covered by plants (m^2 m^{-2})

q_{ac} solar radiation absorbed by the greenhouse cover (W m^{-2})

q_{aspm} solar radiation absorbed by the soil mulch (W m^{-2})

q_{rcNET} net thermal radiation rate at the greenhouse cover (W m^{-2})

q_{rsNET} net thermal radiation rate at the soil (W m^{-2})

q_{sc} heat conducted beneath the polypropylene mulch (W m^{-2})

q_{sjk} soil heat conducted in the soil layer between depth z_j and z_k (W m^{-2})

q_{sky} downward longwave atmospheric irradiance (W m^{-2})

R	specific gas constant, 287 (J kg^{-1}K^{-1})
$\mathrm{Re_p}$	Reynold number (–)
R_g	outside global solar radiation flux density (W m^{-2})
$RMSE$	Root Mean Square Error (ºC)
$RMSPE$	Root Mean Square Percentage Error (%)
R_{Si}	inside global solar radiation flux density (W m^{-2})
R_{Hi}	inside air relative humidity (%)
R_{sz0}	thermal resistance of the polypropylene mulch (m^2 K W^{-1})
S_c	surface area of greenhouse cover (m^2)
S_s	surface area of soil (m^2)
S_{VR}, S_{VS}	roof and the side openings' surface areas (m^2)
t	time (s)
T_i	interior air temperature (K)
T_e	exterior air temperature (K)
T_v	vegetation temperature (K)
T_c	average greenhouse cover temperature (K)
T_{sky}	temperature of sky (K)
T_{spm}	temperature of the polypropylene mulch (K)
T_{sk}	temperature of the soil at depth k (K)
u	air velocity inside the greenhouse (m s^{-1})
U_0	wind speed (m s^{-1})
V_g	greenhouse volume (m^3)
v_V	air velocity through the greenhouse vents (m s^{-1})
w_{Vj}	height of the opening j ($_R$ for roof and $_S$ for side openings) (m)
X_j	value predicted by the model at time j (K)
X_M	mean of values predicted by the model (K)
Y	insect-proof screen inertial factor (–)

Y_j value measured at time j (K)

Y_M mean of values measured (K)

z_k depth in the soil (m)

Greek symbols

α_{ct} cover absorptivity of thermal radiation (–)

α_{cw} absorptivity of the whitened greenhouse cover to global solar radiation (–)

α_{Lpm} long wave radiation absorptivity of the polypropylene mulch covering the soil (–)

α_{Ls} soil surface absorptivity of thermal radiation (–)

α_{pp} polypropylene absorptivity of solar radiation (–)

α_{spm} fraction of the incident solar radiation that is absorbed by the polypropylene mulch covering the soil (–)

α_{Vj} angle of opening (º)

δ_a air density (kg m^{-3})

δ_c greenhouse cover material density (kg m^{-3})

δ_{sik} average density of the soil between depth z_i and z_k (kg m^{-3})

δ_{spm} polypropylene density (kg m^{-3})

ε_c emissivity of greenhouse cover (–)

ε_{spm} emissivity of the polypropylene mulch covering the soil (–)

θ_G angle of incidence of wind (º)

θ_w wind direction (º)

μ_a dynamic viscosity of the fluid (kg s^{-1} m^{-1})

ρ_∞ reflectance of a dense stand (–)

ρ_{cs} downward effective reflectance of the covers (–)

ρ_{cw} reflectance of the whitened cover to solar radiation (–)

ρ_L reflectance of the tomato leaf tissue (–)

ρ_{pl} effective reflectance of the plant layer to solar radiation (–)

ρ_{spm} reflectance of the polypropylene mulch (–)

σ Stefan–Boltsman constant (W m^{-1} K^{-4})

φ insect-proof screen porosity (%)

τ_{cs} downward effective transmittance between the greenhouse cover and the soil (–)

τ_{cw} transmittance of the whitened cover to solar radiation (–)

τ_{cLW} transmittance of the whitened cover to long wave radiation (–)

τ_{ha} transmittance of the humid air due to absorption of water vapour to global solar radiation (–)

τ_{L} transmittance of the leaf tissue (–)

τ_{Lpl} tomato transmittance for diffuse longwave radiation (–)

τ_{pl} transmittance of the plant layer to solar radiation (–)

τ_{Spl} canopy transmittance for diffuse shortwave radiation (–)

1. Introduction

Greenhouses currently constitute the main system to produce high-yield and high-quality horticultural crops almost all year round in the Mediterranean region. Mild winter climatic conditions have allowed the development of more than 278,000 ha of low-plastic tunnel and greenhouses in the Mediterranean region (FranceAgriMer, 2013; Tüzel and Öztekin, 2015), making this the second largest zone in the world after Asia, which is come to more than 4.7 million ha of protected vegetable (Kang et al., 2013; Yang et al., 2014).

Spain had about 52,325 ha of greenhouses in 2014, 21,042 ha of which were occupied by tomato crops (MAGRAMA, 2014). The greatest concentration of greenhouses in the Mediterranean region is located in the province of Almería on the southeast coast of Spain, where a recent satellite imagery analysis put the greenhouse surface area at 30,007 ha (CAPDR, 2016).

Average tomato production in Almería's unheated greenhouses is around 17 kg m^{-2}, with some growers reaching yields of about 21 kg m^{-2} (Valera et al., 2016). These values are below the 55 kg m^{-2} obtained in the high-tech greenhouses of Northern Europe or America (with heating systems), and below the 20-35 kg m^{-2} reached in solar greenhouses in China (Costa et al., 2004).

One of the main problems confronted in the Mediterranean Basin is reduced ventilation resulting in excessively high inside temperatures, typically occurring from May to August (Pardossi et al., 2004). During this period, improving the capacity and control of natural ventilation is a crucial factor in maintaining suitable values of temperature, humidity and CO_2 concentration inside the greenhouse and, therefore, in increasing crop production.

1.1. Microclimate simulations

Modelling of microclimatic parameters is essential to optimise climatic conditions inside greenhouses during different stages of plant growth (Sethi et al., 2013). Simulation models are a good tool to optimize greenhouse ventilation systems, allowing us to predict the inside temperature as a function of outside climatic parameters and greenhouse characteristics.

A greenhouse is a multi-input and multi-output (MIMO) system subject to strong perturbations produced by sudden meteorological variations that need to be taken into account in the models (Lafont et al., 2015). However, it is impossible to describe all internal factors as a function of all external influences, and consequently developing a model requires selection of the relevant system parameters to be estimated and the necessary external data (Bot, 1989a).

Models applied to greenhouses can be divided into two categories: static models for the design of new greenhouses and dynamic models for the climate control of existing structures (Kano and Sadler, 1985). Sethi et al. (2013) reviewed numerous static and dynamic thermal models which describe the microclimate of greenhouses and have been validated in different locations and climates, as well as with different crops. On the other hand, a detailed analysis of advantages and disadvantages of the different control theories applied in greenhouse climate control systems can be found in Duarte-Galvan et al. (2012).

Greenhouse models can also be classified as physical or phenomenological models (white box), purely theoretical and empirical models (black box), which establish relationships between input (outside climate parameters) and output variables (inside climate parameters) without physical significance (Krauss et al., 1997). Classic models of stationary energy balance (Walker, 1965; Kimball, 1973) generally used few parameters as input, whereas modern dynamic models use multiple parameters to describe the greenhouse as they are computer-based, and mathematical optimisation procedures are used to determine the values.

1.2. Physical or phenomenological models

Kindelan (1980) simulated the environment inside a small hydroponic greenhouse by the energy balance method, dividing the system into four elements (soil, plant, inside air and cover). The evolution of temperatures over time was obtained considering only the heat storage in the upper 0.3 or 0.4 m of soil, where the temperature oscillations were appreciable. Bot (1980; 1989b) also developed a dynamic physical model of greenhouse climate based on the energy, water vapour and CO_2 balances of the crop-greenhouse system, using sub-models of radiation transmission and ventilation.

Garzoli (1985) developed a simplified energy balance model based on a linear function of wind speed to estimate the ventilation rate of a greenhouse in Australia. Boulard and Baille (1987) used a single stationary energy balance equation to analyse the thermal performance of two greenhouses (with fan ventilators), based on solar efficiency and including the effect of thermal inertia in the canopy and the soil. This simple thermal balance model was later used to estimate the energy requirement by the decision making system SERRISTE, developed to generate daily climate set points for greenhouse grown tomatoes (Tchamitchian et al., 2006).

Subsequently, Boulard and Baille (1993) improved their first model by incorporating the effects of natural ventilation and evaporative cooling (fog-system). This model was used in warm climate conditions to estimate temperature and relative humidity inside naturally ventilated greenhouses in Argentina (Bouzo et al., 2006) and northern Mexico Reyes-Rosas et al. (2012), involving a thorough investigation into how the parameters used to estimate the renovation rate affect the model's accuracy.

The Gembloux Greenhouse Dynamic Model (GGDM), a dynamic comprehensive one-dimensional thermodynamic energy balance model that calculates heat and mass transfers in greenhouses taking into account the conductive, convective, radiative (solar and thermal) and latent heat energy exchanges between the cover, interior air, crop and four soil layers, resulting in seven differential equations (Deltour et al., 1985), was initially used to compare two types of covers in passive and heated greenhouses (de Halleux et al., 1985).

Some years later, Pieters et al. (1997) enhanced the model by describing in great detail the condensation and evaporation phenomena inside the greenhouse. Subsequently, Wang and Boulard (2000) improved calculations of natural ventilation flux by introducing an experimental non-dimensional ventilation function, validating it in a plastic multispan greenhouse with only roof vents. Recently, this model, extensively validated for tomato crops in European greenhouses, was adapted by Mashonjowa et al. (2013), who included an equation for ventilation in greenhouses with continuous side and roof vents (Kittas et al., 1997) to simulate the microclimate in a naturally ventilated greenhouse containing a rose crop in Zimbabwe.

Fatnassi et al. (2013) developed a dynamic semi-empirical model of the climate of a large naturally ventilated commercial greenhouse in Morocco with tomato crop, based on energy and humidity balances. This model considered the combinations of buoyancy and wind effects to calculate the ventilation flux in greenhouses equipped with insect-proof screens over the vent openings.

Similar models have been developed in recent years to adapt it to the particular conditions of each country. Thus, Abdel-Ghany and Kozai (2006) developed a dynamic simulation model for heat and water vapour transfers in a naturally ventilated greenhouse in Japan, applying unsteady-state energy balances to the four greenhouse components (plastic cover, inside moist air, potted tomato plants and the greenhouse soil mulched with a black plastic sheet). Unlike the models mentioned above, which use functions based on Bernoulli's equation, this model estimated the ventilation rate from the energy balance under steady-state conditions (Mihara and Hayashi, 1978).

Another mathematical model (MICGREEN), based on energy balances in the four same greenhouse components, was developed by Singh et al. (2006) to simulate the microclimate inside a non-ventilated greenhouse in India. Ganguly and Ghosh (2009) developed a single energy balance model to predict the microclimate inside a greenhouse combining side and roof ventilation and growing flowers in India, concluding that inside temperature was significantly influenced by the intensity of solar radiation, the wind speed and the distance between the side and roof vents. The SIMICROC model developed by Briceño-Medina et al. (2011) integrated the two models of Abdel-Ghany and Kozai (2006) and Singh et al. (2006) in a set of five ordinary differential nonlinear first order equations, used to determine the energy and mass balances in a naturally ventilated greenhouse in Venezuela.

1.3. Empirical models

On the other hand, empirical models can be based on simplifications of theoretical models (using optimization techniques to obtain the values of parameters) or in neural networks (establishing a large number of connections between parameters characterising the model) without a theoretical basis. In recent years, considerable attention has been paid to the optimization techniques that reduce the differences between the measured and calculated values of climatic variables. These techniques modify some of the empirical parameters included in the models (such as minimum and maximum stomatal conductance, transmission coefficient of the greenhouse, discharge coefficient C_d or wind effect coefficient C_w).

Boulard et al. (1996) developed an empirical model, based on a complex dynamic model (Deltour et al., 1985) and more simplified models (Garzoli, 1985; Boulard and Baille, 1987), using a system of four mathematical equations representing the heat and water vapour balances. Hasni et al. (2011) used a digital simulation based genetic algorithm (GA) and a particle swarm optimization (PSO) procedure to improve the physical sizes of the model of Boulard et al. (1996). Lammari et al. (2012) also employed the GA technique to optimize a nonlinear model of an environmental greenhouse.

In the same way, Blasco et al. (2007) used GAs to adjust parameters of a non-linear model-based predictive control (MBPC), incorporating energy and water consumptions. Kumar et al. (2010) used a GA optimization technique to adapt the model developed by Boulard and Baille (1993) to a new greenhouse with a Gerbera crop, observing that the width of the side opening and the angle of the roof vent influenced the model's performance considerably.

Seginer et al. (1994) and Seginer (1997) used an artificial neural network (NN), and subsequently Linker and Seginer (2004) modelled the temperature of the greenhouse by using sigmoid neural networks and hybrid models. NN models can be used for environmental control in greenhouses with the advantage of unnecessary explicit evaluation of transfer coefficients (Seginer et al., 1994). He and Ma (2010) developed a NN model based on the Principal Component Analysis (PCA) technique for modelling air humidity inside a greenhouse in northern China during the winter period.

However, results of NN models cannot be extrapolated from one greenhouse to another as they require measurements in each greenhouse to establish the relationship between input and output, and therefore they cannot be used for design purposes. On the contrary, energy balance models can be used to compare several configurations of a greenhouse in different environmental scenarios, for instance the simplified greenhouse environment model incorporated into a web-based application by Fitz-Rodríguez et al. (2010).

Taki et al. (2016) compared a physical dynamic model with a NN model (using inside soil temperature and inside air humidity as inputs) to predict inside air and roof temperatures and energy loss in a semi-solar greenhouse in Iran, obtaining better results with the NN model. More recently, Castañeda-Miranda and Castaño (2017) have also developed a NN model for smart frost control in greenhouses in the central Mexico, with highly accurate temperature predictions (standard error of below 3%). One of the input variables used in these two models was relative air humidity, which depends on inside temperature (and others parameters) and is subsequently considered as a secondary boundary condition. The use of secondary boundary conditions improves the accuracy of estimations but reduces the predictive capacity. To predict the evolution of climate parameters over time inside a specific greenhouse as a function of outside climatological parameters, it is convenient to use a model based only on primary boundary conditions (environmental conditions that are easily measurable and unaffected by the existence of the greenhouse) while also including the heat storage capacity of the soil (Kindelan, 1980).

Thus, the objective of the present work was to develop a dynamic model of energy balance to predict temperatures of air, greenhouse cover and soil coupled with the empirical linear regression obtained by Wang and Deltour (1999) to predict crop temperature using only primary boundary conditions. To estimate these temperatures accurately inside a naturally ventilated greenhouse equipped with screened roof and side vents, the model includes a novel method to calculate the ventilation airflow using variable discharge C_d and wind effect C_w coefficients. The model takes into account the effect of velocity across the screened vents and the wind direction.

2. Materials and methods

2.1. Experimental set-up

For validation of the climate model experimental measurements were conducted in a 24 × 45 m (area S_s=1080 m^2 and volume V_g=6156 m^3) three-span greenhouse (Fig. 1a) oriented in a NW–SE direction (Fig. 1b). This greenhouse is located on the northern limit of the UAL-ANECOOP Foundation's Innovation and Technology Centre "Eduardo Jesús Fernandez Rodriguez" of the University of Almería (longitude: 2°17' W, latitude: 36°51' N and altitude: 90 m above mean sea level). The greenhouse was equipped with three roof windows and two side vent openings with maximum surfaces, S_{VRmax}=116.4 m^2 and S_{VSmax}=84 m^2, respectively (approximately 10.8% and

7.8% of the soil surface area, respectively), all covered with insect-proof screens whose characteristics are given in Table 1.

Table 1.

Geometric and aerodynamic characteristics of the insect-proof screen (López et al., 2016).

Parameter	Value
Thread density, D_r (threads cm^{-1} × threads cm^{-1})	9.6 × 20.3
Porosity, φ (%)	36.0
Screen thickness, e_{scr} (m)	508.1 × 10^{-6}
Permeability, K_p (m^2)	4.215 × 10^{-9}
Inertial factor, Y	0.184

Vent openings were opened automatically when air temperature exceeded 20°C, and closed when wind speed surpassed 8 m s^{-1} by means of the Multima advanced control computer using Synopta software (Hortimax S.L., El Ejido, Spain). The Almería region is characterised by two prevailing winds directed by the Mediterranean basin: the *Levante*, a warm dry north-east wind blowing from the land to the sea and the *Poniente*, a cold damp wind from south-west (Kuciauskas et al., 1998).

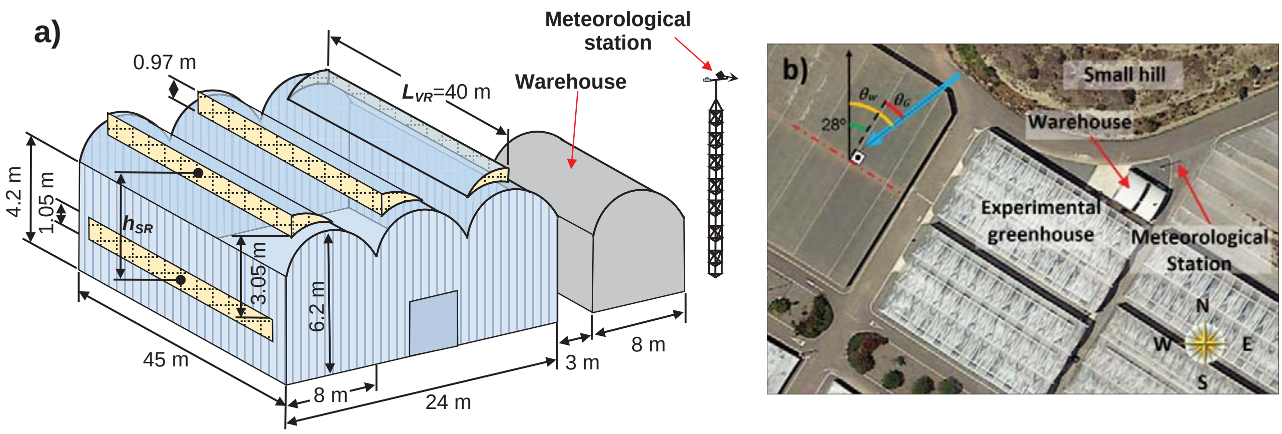

Fig. 1. (a) Dimensions of the experimental greenhouse and (b) neighbouring obstacles.

Natural ventilation was affected by different obstacles surrounding the experimental greenhouse (López et al., 2011). The southern side and the eastern end of the greenhouse were only 3 m away from other multispan greenhouses (6.75 m maximum height, 4.6 m at the gutters). The eastern part of the northern side faced a small warehouse while the western part is located 10 m away from a small hill (Fig. 1b). The greenhouse ceiling (with an area of S_{c1}=1198 m^2) was covered with a 0.2 mm thick three-layer co-extruded film (composed of a layer of ethylene vinyl acetate inserted between two polyethylene films) and the walls (S_{c2}=687.6 m^2) were covered with polycarbonate corrugated sheets.

The greenhouse had an '*arenado*' sand mulch soil, typical of Almería greenhouses (Valera et al. 2016), covered with a black polypropylene sheet (0.225 mm thickness). Woven black polypropylene mulches are often used for weed control (Andersen et al., 2013) and to reduce soil water evaporation (Farina et al., 2003). During the 2014/15 season two soilless tomato crops (*Solanum Lycopersicum* L.) were grown inside the greenhouse on coconut fibre substrate: an autumn-winter crop (cv. Racymo) from September 2014 to January 2015 and a spring-summer crop (cv. Bermello) from February to July 2015.

Different sensors were installed outside and inside the greenhouse (Fig. 2) to measure outside climatic variables used as primary boundary conditions model inputs (solar radiation, air temperature, wind speed and direction), and inside microclimatic parameters used to validate the model. The data from 24 sensors were recorded by three Microloggers CR3000 (Campbell Scientific Spain S.L., Spain).

Climatic parameters outside the greenhouse were recorded by a meteorological station at a height of 10 m (Fig. 1a). The meteorological station incorporated a BUTRON II (Hortimax S.L., Almería, Spain) measurement box with temperature and humidity sensors. The station also included solar radiation and wind speed and direction sensors. To measure inside air temperature T_i and humidity R_{Hi} (Table 2), two sensors were located under each span ridge (at 1 m and 2 m height), two close to the roof windows and two in the middle of the side openings (Fig. 2). Air velocity was measured in the middle of the greenhouse and in the centre of the two side openings with sonic anemometers.

Greenhouse cover, plant and soil temperatures were measured with 12 thermistors. On the outside and inside surfaces of the greenhouse cover, sensors were attached to the plastic surface and protected with a radiation shield (Abdel-Ghany et al., 2006). The sensor used to measure soil surface temperature T_{spm} was attached to the upper face of the polypropylene mulch and the thermistor was covered with a flexible polyethylene sheet to insulate it thermally from inside air. Soil temperature was measured at three different depths (0.01, 0.05 and 0.15 m). Two more thermistors were located between two tomato leaves.

Table 2

Technical characteristics of sensors to measure climate parameters.

Parameter	*Sensor*	*Manufacturer*	*Range*	*Accuracy*
T_i – Inside air temperature	12 × CS215		5 °C -40 °C	±0.4 °C
R_{Hi} – Relative humidity		Campbell Scientific Spain S.L.,	0-100 %	±4%
R_{Si} – Inside solar radiation	2 × SP1110 pyranometer	Barcelona, Spain	350-1100 nm	±5%
R_g – Outside solar radiation				
T_c – Greenhouse cover temperature	10 × Betatherm 100K6A thermistor	Measurement Specialties, Inc., Galway, Ireland	–5 °C-95 °C	±0.49 °C
T_{spm} – Soil surface temperature				
T_{s0} – Soil temperature at 0.01 m				
T_{s1} – Soil temperature at 0.05 m				
T_{s2} – Soil temperature at 0.15 m	TCAV thermocouple	Campbell Scientific Spain S.L.	–40 °C-375 °C	±1.5 °C
q_{sc} – heat flux beneath the mulch	2 × HFP01	Hukseflux Thermal Sensors B.V., Delft, The Netherlands	±2000 W m^{-2}	–15 +5%
q_{s12} – soil heat flux (0.1 m depth)				
u – air velocity inside greenhouse	3 × 2D Windsonic	Gill Instruments, Lymington, UK	0-60 m s^{-1}	±2%
U_o – Outside wind speed	Meteostation II -Cup anemometer	Hortimax S.L., Almería, Spain	0-40 m s^{-1}	±5%
θ_w – Outside wind direction	Vane		0-360°	±5°
T_e – Outside air temperature	Pt1000-BUTRON II	Hortimax S.L., Almería, Spain	–25 °C-75 °C	±0.01 °C
T_v – Leaf temperature	2 × Betatherm 100K6A thermistor	Measurement Specialties, Galway, Ireland	–5 °C-95 °C	±0.49 °C

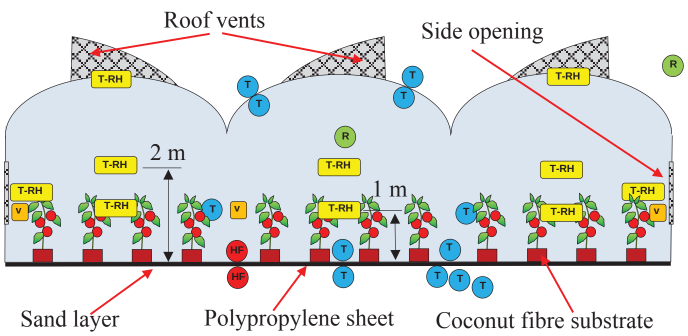

Fig. 2. Distribution of sensors located inside and outside the greenhouse for the measurement of climatic parameters: Temperature and relative humidity sensors (T-RH), pyranometers (R), heat flux plate (HF), thermocouples (T) and wind sonic anemometers (v).

The heat flow by conduction toward the ground was recorded using two soil heat flux plates, one was placed between the plastic mulch and the soil (to measure the heat flux beneath the mulch q_{sc}) and the other at 0.1 m depth (to measure soil heat flux q_{s12}). Solar radiation inside, R_{Si}, and outside the greenhouse, R_g, were measured with two pyranometers (Table 2), which allowed calculation of the cover transmissivity. The thickness of the polypropylene mulch film, e_{spm}, the greenhouse cover, e_c, and the insect-proof screen, e_{scr}, were measured using a TESA-VISIO 300 GL non-contact optical measurement device (TESA SA, Switzerland) with a resolution of 0.05 µm. Precision E_{xy}=2.9+10·e/1000 (µm) depend on the thickness e (mm) of the measured sample.

2.2. Description of the model

The dynamic model developed in this work was based on energy balances in the seven components of the greenhouse system (crop, cover, polypropylene mulch, three soil layers and inside air). This model took into account conductive, convective and radiative (solar and thermal) heat transfers between these greenhouse components and mass transfer by natural ventilation and transpiration (Fig. 3). The evolution over time of air, greenhouse cover, polypropylene mulch and soil temperatures (T_i, T_c, T_{spm}, T_{s0}, T_{s1} and T_{s2}, respectively) was obtained by coupling six energy balance differential equations with an empirical linear regression to predict crop temperature, T_v (Wang and Deltour, 1999). This model only uses primary boundary conditions as input parameters: outside solar radiation R_g, outside air temperature T_e, outside wind speed U_o and direction θ_w.

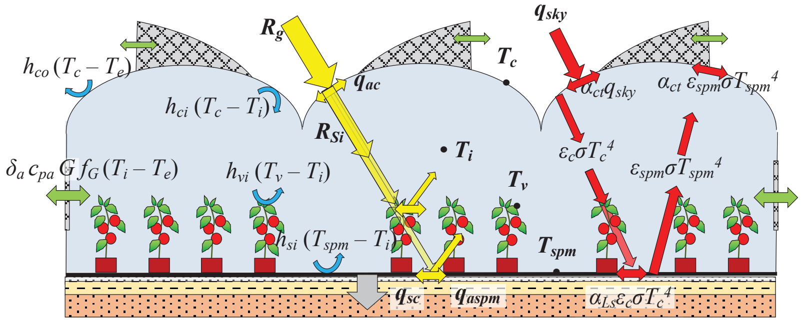

Fig. 3. Heat flux between the different components of the greenhouse model: solar (■) and thermal (■) radiations transmitted and reflected (→) or absorbed (↔), conduction (■), convection (■) and ventilation (■).

Besides the greenhouse component temperatures, the model allows the following output data to be obtained: inside solar radiation, R_{Si}, heat flux beneath the mulch, q_{sc}, soil heat flux, q_{s12} and air velocity through the greenhouse vents, v_V. The model considered the combination of buoyancy and wind effects to estimate the ventilation flow G, calculating different discharge coefficients for roof, C_{dVR}, and side, C_{dVS}, vents as a function of the geometry of the opening, the aerodynamic characteristics of the insect-proof screen (Table 1) and the average velocity of air across the openings (in the previous time interval). The model also took into account the effect of wind direction by using different wind effect coefficients, C_w for *Levante* (NE) and *Poniente* (SW) winds and a coefficient f_G calculated as a function of the wind direction θ_w.

The incident solar energy on the greenhouse R_g is absorbed by the cover q_{ac}, by the water vapour inside the greenhouse, by the plants and by the polypropylene mulch q_{aspm} (Fig. 3). The remaining portion of R_g is lost due to reflection on the external cover surface, on the canopy and on the polypropylene mulch surface. The energy absorbed by the greenhouse cover q_{ac} and the soil mulch q_{aspm} were determined as a function of the geometry considering the multiple reflections for the transmitted radiation between the greenhouse components as proposed by Abdel-Ghany and Al-Helal (2011), rather than constant absorptions of the greenhouse components.

In this model, the following assumptions were made:

a) The air in the greenhouse is well mixed and its temperature is uniform and air exiting the greenhouse by the openings is equal to the average inside air temperature.

b) Air entering the greenhouse is at the same temperature as the outside air, measured at the meteorological station.

c) No evaporation occurs from the soil because of the use of soilless crop and polypropylene mulch.

d) Crop temperature can be estimated accurately from solar radiation and temperature inside the greenhouse.

e) The coconut fibre's contribution to heat storage is negligible.

f) Soil temperature at 0.5 m depth is constant throughout the year.

2.2.1. Crop temperature

A reasonable approximation of the vegetation temperature T_v can be obtained from the interior air temperature T_i and the inside global solar radiation R_{Si} using the multiple linear regression model proposed by Wang and Deltour (1999):

$$T_v = -2.05 + 1.01T_i + 0.00425R_{Si} \qquad (1)$$

Inside global solar radiation flux density was calculated from the outside global solar radiation flux density R_g and the transmissivity τ_{cw} of the greenhouse cover as:

$$R_{Si} = \tau_{cw}R_g \qquad (2)$$

The experimental greenhouse cover was whitened on different dates, and as a result the value of τ_{cw} changed over the crop season (Table 3). This is the most frequently used technique to reduce inside temperature in Spanish greenhouses due to its low cost (Valera et al., 2016).

Table 3

Values of the leaf area index L_{AI} and transmissivity of the greenhouse cover τ_{cw} in five different time periods. Maximum and minimum values of the measured inside air temperature T_i.

	Period	L_{AI} (m^2m^{-2})	τ_{cw}	T_{imax} (°C)	T_{imin} (°C)
1	21-25 Dec 2014	1.30	0.82	22.2	6.9
2	5-9 Jan 2015	0.74	0.82	23.3	6.3
3	15-19 Apr 2015	0.94	0.42	29.1	11.9
4	29 Apr – 3 May	1.10	0.47	31.9	13.4
5	1-5 Jun 2015	0.92	0.47	36.9	17.2

2.2.2. Greenhouse cover temperature

The greenhouse cover temperature T_c was calculated by means of a first-order differential equation (Joudi and Farhan, 2015):

$$\delta_c c_{pc} e_c \frac{dT_c}{dt} = q_{ac} + q_{rcNET} - h_{ci}(T_c - T_i) - h_{co}(T_c - T_e) \qquad (3)$$

where δ_c is the greenhouse cover material density (kg m^{-3}), c_{pc} the specific heat of the greenhouse cover material (J kg^{-1} K^{-1}), e_c the cover thickness (m), q_{ac} the solar radiation absorbed by the greenhouse cover (W m^{-2}) and q_{rcNET} the net thermal radiation rate at the greenhouse cover (W m^{-2}). The last two terms are the energy transferred by convection between the greenhouse cover and the inside and outside air, respectively (Fig. 3).

According to Joudi and Farhan (2015) the solar radiation absorbed by the greenhouse cover can be calculated using the following equation:

$$q_{ac} = \alpha_{cw} R_g \left(1 + \left(1 - \propto_{spm}\right)\right) \qquad (4)$$

where α_{cw} is the absorption coefficient of the whitened greenhouse cover (Table 4).

Considering multiple reflections of the transmitted fraction τ_{cs} between the soil surface and the lower surface of the greenhouse covers, the absorbed fraction of solar radiation in the polypropylene mulch covering the greenhouse soil can be calculated as (Abdel-Ghany and Al-Helal, 2011):

$$\alpha_{spm} = \frac{(1 - \rho_{spm})\tau_{cs}}{(1 - \rho_{spm}\rho_{cs})} \qquad (5)$$

where the reflectance of the polypropylene mulch ρ_{spm}=0.05 was calculated from its absorptivity $\rho_{spm}=1-\alpha_{pp}$ (Table 4).

The downward effective transmittance between the greenhouse cover and the soil was calculated as (Abdel-Ghany and Al-Helal, 2011):

$$\tau_{cs} = \frac{\tau_{cw}\tau_{ha}\tau_{pl}}{(1 - \rho_{pl}\rho_{cw}\tau_{ha}^2)} \qquad (6)$$

The reflectance of the greenhouse cover to global solar radiation was calculated as:

$$\rho_{cw} = 1 - \alpha_{cw} - \tau_{cw} \qquad (7)$$

where the absorptivity of the whitened greenhouse cover to global solar radiation α_{cw} was considered as constant (Table 2) and the transmissivity changed depending on the whitening level (Table 3).

Water vapour is the most important absorber in air (Nwoye et al., 2014), and humid air transmissivity τ_{ha} can be calculated as a function of length of beam L_b [m] and relative air humidity R_{Hi} [%] as (Brzustowski and Sommer, 1973):

$$\tau_{ha} = 0.79\left(\frac{3280}{R_{Hi}L_b}\right)^{\frac{1}{16}} \qquad (8)$$

Although the length of beam inside the greenhouse changes throughout the day depending on the angle of incidence of solar radiation on the greenhouse cover, we have used a constant value of L_b=15.1 m (average of the maximum height and width of the greenhouse). With a view to using only primary boundary conditions in the model, we have calculated a constant value of τ_{ha}=0.86, corresponding to an inside relative humidity of R_{Hi}=60%.

In future, this model could be coupled to a water vapour balance model, thus allowing the use of Eq. (8) with variable values of R_{Hi}.

Table 4

Values of the model parameters used in the simulation.

	Parameter (Unit)	Symbol	Value	Source
Greenhouse cover	Plastic thickness (m)	e_c	0.002	Measured
	Absorptivity of PE-EVA-PE to solar radiation	α_{cw}	0.03	Nijskens et al., 1984
	Emissivity of cover to long wave radiation	$\varepsilon_c = \alpha_{ct}$	0.59	Feuilloley et al., 1990
	Cover transmissivity to long wave radiation	τ_{cLW}	0.38	Feuilloley et al., 1990
	Cover specific heat (J Kg^{-1} K^{-1})	c_{pc}	2302	Zarandi and Bioki, 2013
	Cover density (kg m^{-3})	δ_c	1150	Sengar and Kothari, 2008
Polypropylene mulch	Polypropylene sheet thickness (m)	e_{spm}	0.0025	Measured
	Polypropylene density (kg m^{-3})	δ_{spm}	890	Wypych, 2016; Puszkarz et al., 2016
	Polypropylene specific heat (J Kg^{-1} K^{-1})	c_{spm}	1881	Puszkarz *et al.*, 2016
	Polypropylene absorption to solar radiation	α_{pp}	0.95	Kurzböck et al., 2012
	Emissivity of the polypropylene	ε_{spm}	0.95	Yannas et al., 2006
	Mulch absorption to thermal radiation	α_{Lpm}	0.95	Assumed $\alpha_{Lpm} = \varepsilon_{spm}$
	Thermal resistance (m^2 K W^{-1})	R_{sz0}	0.14	Measured
Soil	Temperature of soil at depth z_{s3}=0.5 m (ºC)	T_{s3}	24	Estimated
	Density of sand-soil layer 1 (kg m^{-3})	δ_{s01}	1700	Measured
	Density of clay loam-soil layer 2 (kg m^{-3})	δ_{s12}	1450	Measured
	Density of sandy clay-soil layer 3 (kg m^{-3})	δ_{s23}	1500	Measured
	Specific heat of soil layer 1 (J Kg^{-1} K^{-1})	c_{p01}	800	Hamdhan and Clarke, 2010
	Specific heat of soil layer 2 (J Kg^{-1} K^{-1})	c_{p12}	1900	Joudi and Farhan, 2015
	Specific heat of soil layer 3 (J Kg^{-1} K^{-1})	c_{p23}	1696	Hamdhan and Clarke, 2010
	Thermal conductivity of soil layer 1 (W m^{-1} K^{-1})	k_{s01}	0.27	Hamdhan and Clarke, 2010
	Thermal conductivity of soil layer 2 (W m^{-1} K^{-1})	k_{s12}	0.48	Abu-Hamdeh and Reeder, 2000
	Thermal conductivity of soil layer 3 (W m^{-1} K^{-1})	k_{s23}	1.61	Nikiforova et al., 2013
Tomato crop	Transmittance of the leaf tissue	τ_L	0.20	Stanghellini, 1987
	Reflectance of the tomato leaf tissue	ρ_L	0.28	Monteith and Unsworth, 2008
	Reflectance of a dense tomato stand	ρ_∞	0.12	Stanghellini, 1987
	Extinction coefficient for conical leaf distribution	k_L	0.87	Monteith and Unsworth, 2008
	Characteristic leaf length of the tomato crop (m)	L_{cl}	0.14	Measured

The downward effective reflectance of the greenhouse cover can be estimated as (Abdel-Ghany and Al-Helal, 2011):

$$\rho_{cs} = \rho_{pl} + \frac{\rho_{cw}\tau_{Spl}^{2}\tau_{ha}^{2}}{\left(1 - \rho_{pl}\rho_{cw}\tau_{ha}^{2}\right)} \qquad (9)$$

The effective reflectance of the crop was calculated as the reflection of radiation produced by a dense plant stand, resulting from the reflections of the foliage and underlying soil surface (Stanghellini, 1987):

$$\rho_{pl} = \rho_{\infty}\left(1 - \tau_{Lpl}\right) + \tau_{Spl}^{2}\rho_{spm} \qquad (10)$$

where ρ_{∞} is the reflectance of a dense stand and ρ_{spm} is that of the underlying soil surface covered by the polypropylene mulch. For a tomato crop we have considered the value of ρ_{∞}=0.12 used by Stangellini (1987).

The transmittance of a tomato crop for diffuse longwave radiation is affected only by the geometrical properties of the canopy and can be calculated as a function of the leaf area index L_{AI} as (Stangellini, 1987):

$$\tau_{Lpl} = \exp\left(-k_L L_{AI}\right) \qquad (11)$$

The extinction coefficient can be calculated as a function of the leaf angle distribution. For a conical distribution with an angle of 30º k_L=0.87 (Monteith and Unsworth, 2008; Abdel-Ghany and Al-Helal, 2011).

The transmittance of a canopy for diffuse shortwave radiation can be represented accurately as (Stangellini, 1987):

$$\tau_{Spl} = \exp\left(-k_s L_{AI}\right) \qquad (12)$$

The extinction coefficient for shortwave radiation can be estimated as a function of the optical properties of the leaves as (Goudriaan, 1977; Stangellini, 1987):

$$k_s = k_L\left[\left(1 - \tau_L\right)^2 - \rho_L^2\right]^{0.5} \qquad (13)$$

where τ_L and ρ_L are the transmittance and reflectance of the leaf tissue, respectively, with typical values of τ_L=0.20 (Stanghellini, 1987) and ρ_L=0.28 (Monteith and Unsworth, 2008). With these values the resulting extinction coefficient for the tomato canopy was k_s=0.65.

The longwave net radiative energy flux on the greenhouse cover can be calculated as (Kittas, 1986; Singh et al., 2006; Joudi and Farhan, 2015):

$$q_{rcNET} = \left(-\varepsilon_c \sigma T_c^4 S_c + \propto_{ct} q_{sky} S_c + \propto_{ct} \varepsilon_{spm} \sigma T_{spm}^{4} S_s\right)/S_s \quad (14)$$

where ε_c represents the emissivity of the greenhouse cover (Table 4), σ the Stefan-Boltzmann constant (5.67×10^{-8} W m^{-1} K^{-4}), S_c the surface area of greenhouse cover (m^2), α_{ct} the cover absorptivity of thermal radiation (Table 4), ε_{spm} the emissivity of the polypropylene mulch (Table 4), T_{spm} the temperature of the polypropylene mulch covering the soil (K) and S_s the surface area of soil (m^2).

In Eq. (14), the first term represents the thermal radiation emitted by the greenhouse cover, the second is the atmospheric thermal irradiance absorbed by the cover material and the last term is the thermal radiation emitted by the polypropylene mulch and absorbed by the greenhouse cover (Fig. 3).

The downward longwave atmospheric irradiance incident on the greenhouse cover surface q_{sky} can be calculated according to the following equation (Swinbank, 1963; Pieters et al., 1997; Iziomon et al., 2003; Abdel-Ghany and Kozai, 2006):

$$q_{sky} = A_1 T_e^{\ 6} \tag{15}$$

where A_1=5.31×10^{-13} W m^{-2} K^{-6}.

The convective heat transfer coefficient between interior air and greenhouse cover was calculated, considering the inside airflow as turbulent, according to Fatnassi et al. (2013) as:

$$h_{ci} = 1.75\left|T_c - T_i\right|^{1/3} \tag{16}$$

The values of the convection heat transfer coefficient between outside air and greenhouse cover was calculated as a function of the wind speed U_0 as (Garzoli and Blackwell, 1981):

$$h_{co} = 7.2 + 3.8U_0 \tag{17}$$

2.2.3. Soil temperature

In the present study the greenhouse floor was covered by a black polypropylene mulch that affects heat transfer in the soil. The plastic mulch increases the absorption of solar radiation and the emission of infrared radiation of a bare sandy soil.

The temperature of the mulched top soil T_{spm} was calculated from the first-order differential equation derived from the energy balance in the polypropylene mulch covering the soil:

$$\delta_{spm} c_{spm} e_{spm} \frac{dT_{spm}}{dt} = q_{aspm} - h_{si}\left(T_{spm} - T_i\right) - q_{sc} - q_{rsNET} \tag{18}$$

The outside solar radiation absorbed by the polypropylene surface after multiple reflections of the transmitted fraction by the greenhouse cover, the humid air and the canopy was calculated as:

$$q_{aspm} = \alpha_{spm} R_g \qquad (19)$$

The heat transferred between the soil surface and the inside air was estimated using the coefficient h_{si} calculated according to the following equation (Fatnassi et al., 2013):

$$h_{si} = 1.75 \left| T_{spm} - T_i \right|^{1/3} \qquad (20)$$

The heat conducted from the soil surface at temperature T_{spm} to the soil beneath the polypropylene mulch (Fig. 4) at a depth of z_0=0.01 m and temperature T_{s0} can be estimated as:

$$q_{sc} = \frac{(T_{spm} - T_{s0})}{R_{sz0}} \qquad (21)$$

The thermal resistance R_{sz0} ($m^2\ K\ W^{-1}$) of the polypropylene mulch and the air trapped between it and the soil surface was experimentally determined from measurements of T_{spm}, T_{s0} and q_{sc} (Table 2).

From the energy balances in the different layers of soil (Fig. 4) we can obtain the temperatures of soil T_{sj} at depth z_j as proposed by Joudi and Farhan (2015):

$$\delta_{s01} c_{s01} e_{s01} \frac{dT_{s0}}{dt} = \frac{(T_{spm} - T_{s0})}{R_{sc,z0}} - \frac{k_{s01}(T_{s0} - T_{s1})}{e_{s01}} \quad 0.01 < z \leq 0.05m \qquad (22)$$

$$\delta_{s12} c_{s12} e_{s12} \frac{dT_{s1}}{dt} = \frac{k_{s01}(T_{s0} - T_{s1})}{e_{s01}} - \frac{k_{s12}(T_{s1} - T_{s2})}{e_{s12}} \quad 0.05 < z \leq 0.1m \qquad (23)$$

$$\delta_{s23} c_{s23} e_{23} \frac{dT_{s2}}{dt} = \frac{k_{s12}(T_{s1} - T_{s2})}{e_{s12}} - \frac{k_{s23}(T_{s2} - T_{s3})}{e_{s23}} \quad 0.1 < z \leq 0.5m \qquad (24)$$

where T_{sj} is the soil temperature at depth z_j (K), δ_{sjk} the average density of the soil layer between depths z_j and z_k (kg m^{-3}), c_{sjk} the specific heat of the soil (J kg^{-1} K^{-1}) and e_{sik} its thickness (m). The term T_{s3} is the temperature of soil at z_3=0.5 m (Table 4), at which soil temperature is considered constant throughout the year (Abdel-Ghany and Kozai, 2006).

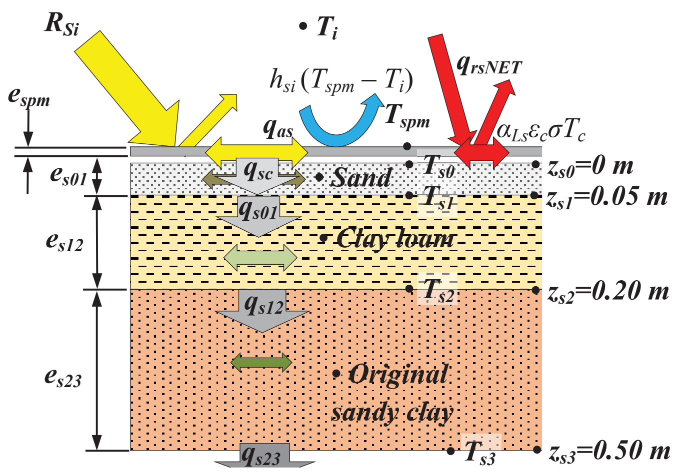

Fig. 4. Heat transfers in the greenhouse soil.

The net radiative heat exchange on the soil surface q_{rsNET} was calculated as (Joudi and Farhan, 2015):

$$q_{rsNET} = \left(- \varepsilon_{spm} \sigma T_{spm}^{4} S_s + \alpha_{Ls} \varepsilon_c \sigma T_c^4 S_c \right) / S_s \qquad (25)$$

The soil surface absorptivity to thermal radiation was calculated as a function of the absorption coefficient of the polypropylene mulch α_{Lpm}=ε_{spm} (Table 4) and the transmittance of the crop for longwave radiation [Eq. (11)]:

$$\alpha_{Ls} = \alpha_{Lpm}\ \tau_{Lpl} \qquad (26)$$

2.2.4. Air temperature inside the greenhouse

Estimation of temperature of inside air T_i is based on the energy balance computing the sensible heat fluxes exchanged between the air and the other components of the greenhouse (Fatnassi et al. 2013):

$$\delta_a c_{pa} \frac{V_g dT_i}{S_s\ dt} = P_v L_{AI}\ h_{vi}\left(T_v - T_i\right) - h_{si}\left(T_i - T_{spm}\right) - \frac{S_c}{S_s} h_{ci}\left(T_i - T_c\right) - \delta_a c_{pa} \frac{G}{S_s} f_G\left(T_i - T_e\right) \qquad (27)$$

where δ_a is the air density (kg m^{-3}), c_{pa} the specific heat of the air inside the greenhouse (J kg^{-1} K^{-1}), V_g the greenhouse volume (m^3) and P_v=0.725 the proportion of area covered by plants (m^2 m^{-2}). In the experimental greenhouse there were 783 tomato plants with a distance of 2.0 m between rows and 0.5 m between plants, resulting in 783 m^2 of soil covered by plants, and a total surface area of soil of S_s=1080 m^2 (including the uncropped border and the concrete corridor in the middle of the greenhouse). The second term in Eq. (27) is the sensible heat transferred between the crop and the inside air, and the last term represents the sensible heat exchange by ventilation with the outside environment (assuming that the air exits the greenhouse with a temperature T_i).

The convective heat transfer coefficient between inside air and plants was calculated as suggested by Fatnassi et al. (2013):

$$h_{vi} = 1.4\left(\frac{\left|T_v - T_i\right|}{L_{cl}}\right)^{0.25} \qquad (28)$$

where L_{cl} is the characteristic leaf length (Table 4).

The volume flow rate exchanged between the inside and outside was calculated considering the sum of two independent pressure fields (induced by buoyancy forces and by wind forces). For a greenhouse equipped with side and roof openings we can use (Pearson and Owen, 1994; Kittas et al., 1997):

$$G = \left[\left(\frac{1}{\frac{1}{C_{dVR}{}^2 S_{VR}{}^2} + \frac{1}{C_{dVS}{}^2 S_{VS}{}^2}} \right) \left(2g \frac{|T_i - T_e|}{T_e} H_{SR} \right) + \left(\frac{C_{dVR} S_{VR} + C_{dVS} S_{VS}}{2} \right)^2 C_w U_o{}^2 \right]^{0.5} \quad (29)$$

where S_{VR} and S_{VS} are the roof and the side openings' surface areas, respectively (m^2), g is the gravitational constant (m s^{-2}), H_{SR} the vertical distance (Fig. 1a) between the midpoint of side and roof openings (m) (Appendix A) and U_o the wind speed (m s^{-1}). We have used a wind effect coefficient C_w of 0.150 for wind coming from the North (118º>θ_w>332º) and of 0.177 for wind from the South (López, 2010). We have used different values of the roof C_{dVR} and side C_{dVS} vent discharge coefficients varying as a function of the air velocity through the vents (Appendix B).

The ventilation flux was adjusted using a coefficient f_G that varies from 1 for winds perpendicular to the greenhouse vents (θ_G=0º) to 0.25 for parallel winds (θ_G=90º). An empirical correlation between f_G and the angle of incidence θ_G was deduced from data supplied by Shklyar and Arbel (2004):

$$f_G = 4.62 \cdot 10^{-8} \theta_G{}^4 - 9.87 \cdot 10^{-6} \theta_G{}^3 + 0.00058 \cdot 10^{8} \theta_G{}^2 + 0.0024 \theta_G + 0.247 \quad (30)$$

The angle of incidence was calculated as a function of the wind direction θ_w and the direction of the greenhouse ridge (Fig. 1b):

$$\theta_G = \theta_w - 28^{\circ} \quad \text{if } \theta_w > 28 \qquad \theta_G = \theta_w + 332^{\circ} \quad \text{if } \theta_w < 28^{\circ} \qquad (31)$$

2.3. Solution Method for the Model

Equations (3), (18), (22), (23), (24) and (27) represent a system of 6 non-linear first order differential equations. The solution of these equations provides the evolution over time of temperatures of inside air T_i, greenhouse cover T_c, polypropylene mulch T_{spm} and soil T_s. The measured values of temperatures at time t=0 s were used as initial conditions. Although the climatic variables were measured inside the greenhouse every minute, the time step considered in the calculation of the model was Δt=300 s (5 minutes), used by the climatic control system installed in the experimental greenhouse to measure the outside climatic variables (wind speed and direction).

The ordinary differential equations were solved numerically using the algorithm LSODA (Soetaert et al., 2010) with a specific program written in the statistical code R. This code is an integrated suite of software facilities for data management, calculation and graphical presentation of results (Venables and Smith, 2016).

2.4. Statistical analysis of the model

In order to predict the accuracy of the model we have calculated the coefficient of determination that in simple regression is equivalent to the square of the correlation coefficient (Kottegoda and Rosso, 2008):

$$R^2 = \frac{\left[\sum_{j=1}^{n}(Y_j - Y_M)(X_j - X_M)\right]^2}{\left[\sum_{j=1}^{n}(Y_j - Y_M)^2\right]\left[\sum_{j=1}^{n}(X_j - X_M)^2\right]} \qquad (32)$$

where n is the number of measurements, Y_M is the mean of the measured values, Y_j is the measured value at time j, X_M is the mean of the predicted values and X_j is the value predicted by the model at time j.

The most commonly used statistics to estimate deviation of the values calculated by models with respect to those measured experimentally is the Root Mean Square Error, RMSE (Kobayashi and Salam, 2000; Shcherbakov et al., 2013):

$$\mathrm{RMSE} = \sqrt{\frac{1}{n}\sum_{j=1}^{n}\left(Y_j - X_j\right)^2} \qquad (33)$$

However, this statistic presents the drawback of scale dependence (Hyndman and Koehler, 2006), measured in ºC for temperature data. To avoid this inconvenience, the accuracy of the developed model was also evaluated using the Root Mean Square Percentage Error (RMSPE) defined as (Shcherbakov et al., 2013):

$$\mathrm{RMSPE} = \frac{100}{Y_M}\sqrt{\frac{1}{n}\sum_{j=1}^{n}\left(Y_j - X_j\right)^2}\ (\%) \qquad (34)$$

3. Results and discussion

3.1. Model validation

The accuracy of the model was tested by comparing calculated temperatures with values measured in the experimental greenhouse (Fig. 2). The parameters characterising the five greenhouse components (air, cover, crop, mulch and soil) and initial conditions at time t=0 s (Table 4) were introduced in the model formed by equations (1) to (31). The accuracy of the model for estimating greenhouse component temperatures was evaluated over 5 non-successive periods of 5 days during the season, from 21 December 2014 to 6 June 2015. The transmissivity of the cover varied between 0.42 and 0.82 (Table 3) for the whitened (April to June) and unwhitened covers (December to February), respectively (Fig. 5a).

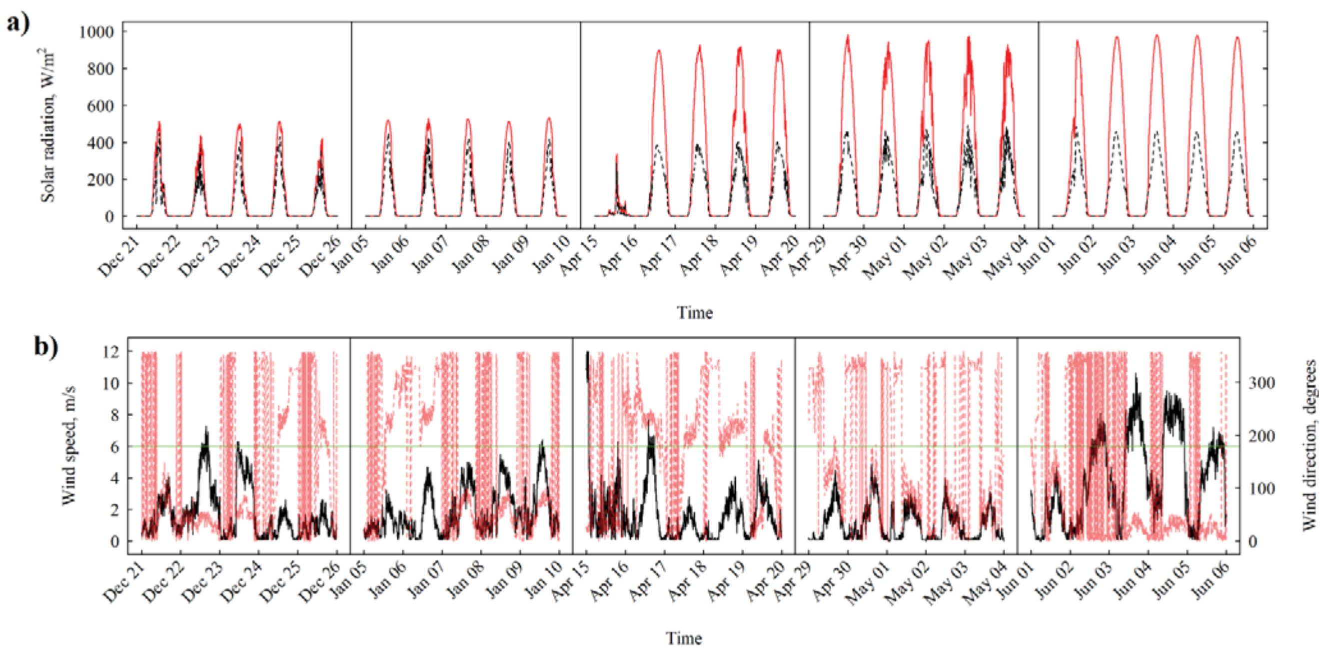

Fig. 5. Outside R_g (—) and inside R_{Si} (---) global solar radiation flux density during the five non-successive periods. (a). Evolution of wind speed U_0 (–) and direction θ_w (---) for the 25 days analysed, and wind-speed limit to begin to close windows (—) (b).

Whitening limits the energy supply from the solar radiation inside the greenhouse. Similar values of global solar radiation were observed inside the greenhouse in winter (21 December to 10 January) without whitening that in spring with whitening (Fig. 5a). Cover whitening is an inexpensive climate control technique that has positive effects on both microclimate and crop behaviour (Baille et al., 2001). Climatic conditions used as primary boundary conditions include a wide range of outside temperatures, from 4 to 33 ºC (Fig. 6). Maximum solar radiation ranged from 514 W m^{-2} at the beginning of the winter, to 973 W m^{-2} at the end of the spring, with values of 360 W m^{-2} on cloudy days (Fig. 5a). The level of whitening changed depending on the time since application and the loss of pigment produced by rain and wind.

Crop growth and leaf pruning resulted in different values of leaf area index in each period, ranging between 0.74 and 1.30 m^2 m^{-2} (Table 3). The predictions of temperature obtained for the five greenhouse components analysed were compared with the measured data. The comparisons were made graphically to show when the differences were greatest (Figs. 6 & 7). To quantify the accuracy of the model and compare it with published greenhouse models, various statistical parameters were used, such as adjusted determination coefficient (R^2), Root Mean Square Error (RMSE) and Root Mean Square Percentage Error (RMSPE), calculated for each period of five days and for the 25 days as a whole (Table 5).

Table 5

Slopes and coefficients of determination R^2 of the correlation lines between measured and calculated values, Root Mean Square Error (RMSE), Root Mean Square Percentage Error (RMSPE) for temperatures of inside air T_i, crop T_v, greenhouse cover T_c, polypropylene mulch T_{spm}, soil surface below the mulch T_{s0} and soil at 0.05 m depth T_{s1} in the five periods analysed.

Periods		***Inside air temperature – T_i***				***Crop temperature – T_v***				***Greenhouse cover temperature – T_c***			
		Slope	R^2	RMSE (ºC)	RMSPE (%)	Slope	R^2	RMSE (ºC)	RMSPE (%)	Slope	R^2	RMSE (ºC)	RMSPE (%)
1	21-25 Dec 2014	0.94	0.97	0.8	6.9	0.95	0.98	0.7	5.7	0.86	0.98	1.1	8.5
2	5-9 Jan 2015	0.88	0.97	1.0	10.3	0.90	0.97	1.0	7.8	0.86	0.98	1.3	10.0
3	15-19 Apr 2015	0.95	0.94	1.1	6.2	0.70	0.89	2.7	14.0	0.67	0.96	3.5	17.5
4	29 Apr-3 May 2015	1.11	0.97	1.5	6.3	1.11	0.92	1.6	7.4	0.82	0.96	2.7	12.6
5	1-5 Jun 2015	0.96	0.96	1.4	4.8	1.05	0.96	1.2	4.9	0.82	0.98	2.2	8.2
	1 - 5	**1.01**	**0.98**	**1.2**	**6.5**	**0.95**	**0.95**	**1.6**	**8.8**	**0.88**	**0.95**	**2.3**	**12.4**
		Polypropylene temperature - T_{spm}				***Soil surface temperature – T_{s0}***				***Soil temperature at 0.05 m – T_{s1}***			
1	21-25 Dec 2014	1.14	0.96	1.0	6.2	0.94	0.94	0.6	3.5	0.68	0.79	0.8	4.7
2	5-9 Jan 2015	1.06	0.92	1.3	8.1	0.98	0.93	0.8	5.3	0.79	0.84	0.9	5.8
3	15-19 Apr 2015	1.08	0.92	2.1	9.2	1.02	0.90	1.5	6.6	1.22	0.83	1.7	7.6
4	29 Apr-3 May 2015	1.16	0.95	2.8	11.2	1.01	0.87	2.3	9.3	1.20	0.79	2.2	9.4
5	1-5 Jun 2015	1.32	0.97	4.8	16.8	0.96	0.93	3.1	10.6	1.24	0.86	3.1	11.2
	1 - 5	**1.24**	**0.96**	**2.8**	**12.8**	**1.10**	**0.96**	**1.9**	**8.8**	**1.18**	**0.97**	**1.9**	**9.1**

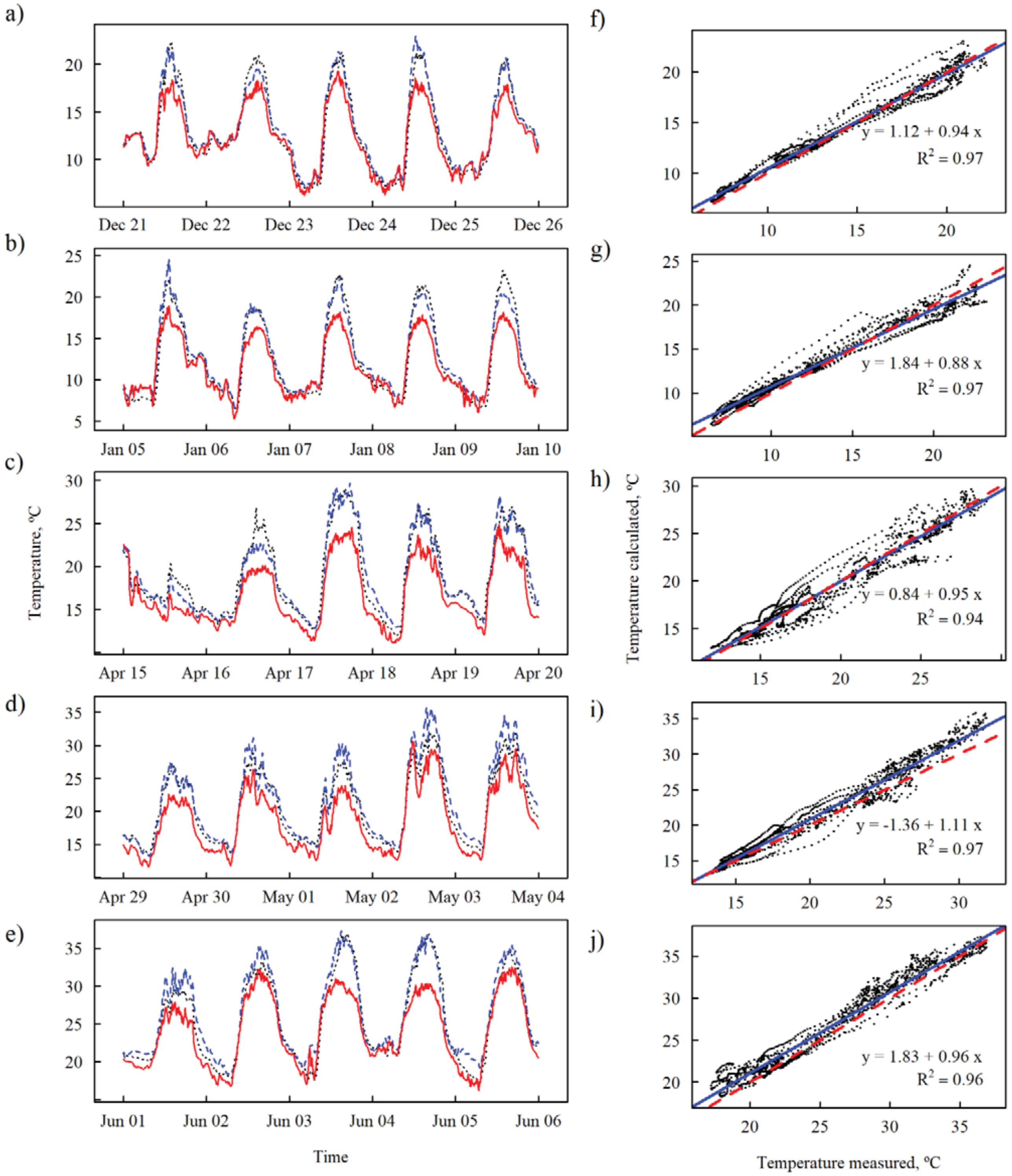

Fig. 6. Evolution of the outside T_e (——) and the inside air temperatures T_i measured (•••••) and calculated (- - -) in five time periods: 21-25 December 2014 (a), 5-9 January 2015 (b), 15-19 April 2015 (c), 29 April – 3 May 2015 (d) and 1-5 June 2015 (e). Relationship between measured and calculated values (○) of inside temperature T_i for each time period (f-j): The dashed line is the line of identity (- - -), and the solid line (—) is the linear regression line (slope, intercept and R^2).

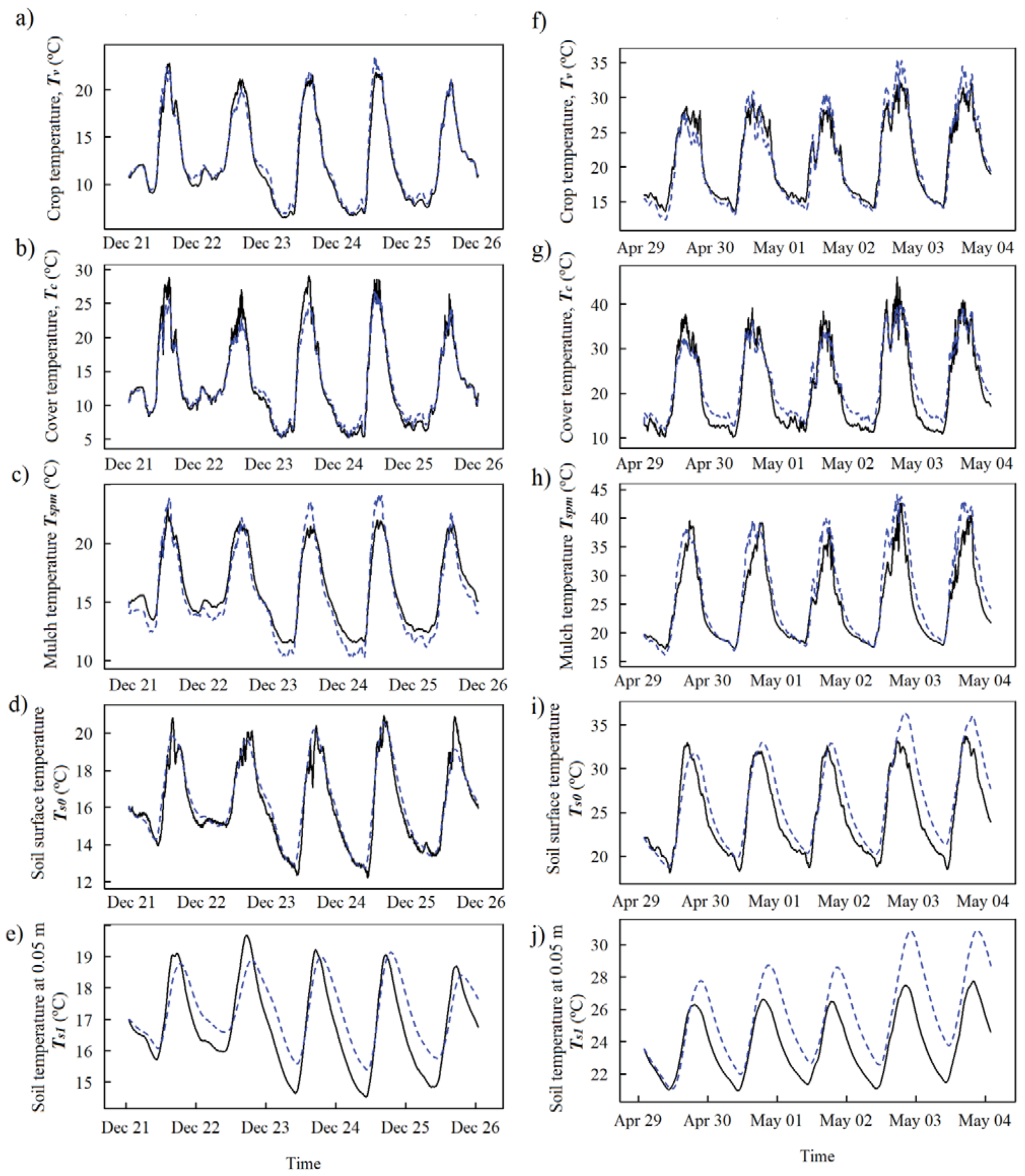

Fig. 7. Evolution of the measured (——) and calculated (- - -) values of temperatures of crop T_v, (a & f), greenhouse cover T_c (b & g), polypropylene mulch T_{spm} (c & h), soil surface below the mulch T_{s0} (d & i) and soil at 0.05 m depth T_{s1} (e & j), in two of the periods analysed: 21-25 December 2014 (a-e) and 29 April – 3 May 2015 (f-j).

The slopes (0.88-1.11) and intercept (–1.36-1.84), with determination coefficient R^2=0.94-0.97, for the linear regression equations relating calculated to measured values of T_i were close to the line of identity (slope=1 and intercept=0) for the five time periods analysed (Fig. 6). Wang and Boulard (2000) obtained slopes of 0.77 (R^2=0.90) and 0.91 (R^2=0.87) for the first soil layer and the interior air, respectively. Fatnassi et al. (2013) also obtained similar results, with a slope of 0.91 (R^2=0.88) for inside temperature.

Values of RMSPE (Table 5) show a good agreement between calculated and measured T_i values over a large range of outside climate conditions (Fig. 5). Mashonjowa et al. (2013) reported values of the mean standard errors between the calculated and measured air and crop temperatures of 1.8 ºC and 1.9 ºC, respectively, using a modified version of the Gembloux Dynamic Greenhouse Climate Model (GDGCM) to model the microclimate of a commercial greenhouse in Zimbabwe.

These values are similar to those of RMSE obtained in the present work of 1.2 ºC for air and 1.6 ºC for crop temperature. These errors are greater than those obtained by other authors (between 0.5 and 1.0 ºC) using the same model (GDGCM) for the spring period with inside temperature ranging from 15 to 25 ºC in Holland (Deltour et al., 1985; Pieters et al., 1997) and France (Wang and Boulard, 2000). Baptista et al. (2010) also tested on spring days, with inside temperature ranging between 15 to 25 ºC in a greenhouse in Portugal, to validate a dynamic climate model and obtained RMSE values of 1.6 ºC, 2.2 ºC and 2.8 ºC for temperatures of inside air, tomato crop and greenhouse cover, respectively. Blasco et al. (2007) observed maximum differences between measured and calculated inside temperature values of 3.5 ºC for summer days with an inside temperature range of 17-33 ºC.

In countries of Central Europe with a lower influence of the ventilation flux in the energy balance, errors in estimation of this flux have a lower influence on the computation of inside air temperature. Estimation of the heat flux exchanged by ventilation with Eq. (27) presents two main problems: inaccuracy in the estimation of the renewal air flow G with Eq. (29) and differences between the temperature of air exiting the greenhouse (needed to compute the loss of energy by ventilation) and the average temperature inside the greenhouse, which are assumed to be equal in Eq. (27). Thus, the accuracy for estimating the quantity of air exchanged by ventilation is lower than for other parameters characterising the greenhouse. This was also observed by Mashonjowa et al. (2013), who obtained values of R^2=0.80-0.81 for the calculation of air renewal rates. On the other hand, the temperature of air exiting the greenhouse via roof vents can be very different to the average inside temperature (Molina-Aiz et al., 2012).

Results from Table 5 and Figs. 6 and 7 show an overall reasonable agreement between predicted and measured temperatures for the five greenhouse components analysed. The best results were obtained for air T_i and soil surface temperature T_{s0}, with RMSPE of less than 10.6% for the five time periods analysed (Table 5). Time evolution of inside air temperature and experimentally measured values were similar for all five periods (Fig. 6). Estimated crop temperature with the multiple linear regression reported by Wang and Deltour (1999) showed a good agreement with measured values (Fig. 7 a & f) with an overall RMSE=1.6 ºC (RMSPE=8.8%) (Table 5). The use of the regression proposed by Wang and Deltour (1999) to estimate crop temperature T_v allows a more simplified model, as it does not require estimation of the stomatal and aerodynamic resistance considered in most models (Baptista et al., 2010; Fatnassi et al., 2013; Mashonjowa et al., 2013).

Simulated greenhouse cover temperatures T_c showed a good agreement with measured values (Figs. 7 b & g). Calculated values of T_c on spring nights (Fig. 7g) were 1-2 ºC greater than measured ones. However, this discrepancy was not observed in winter (Fig. 7b). The overall accuracy of the model in estimation of T_c was better (RMSE=2.3 ºC) than those reported by other models, with RMSE=3.9 ºC (Singh et al., 2006; Briceño-Medina et al., 2011).

Black polypropylene film increased the solar energy absorbed by the soil and the energy transferred to the air by convection, as a consequence of the greater solar absorption coefficient α_{spm}=0.95 than the sandy bare soil α_s=0.65 traditionally used in Spanish greenhouses. The black mulch therefore has a positive effect on cold autumn and winter days. During cold nights, the use of the black mulch increased the amount of heat stored in the soil that is restored to the air by convection.

However, due to the greater emissivity of the black mulch than the sandy bare soil, mulch increases the loss of energy by longwave radiation. Calculated values of polypropylene mulch T_{spm} on winter nights were about 1 ºC lower than the measured ones (Fig. 7c), although in spring a good agreement can be observed (Fig. 7h). Estimated values of T_{spm} showed good agreement with measurements in the morning and evening. However, the model predicted greater temperature oscillations than those measured experimentally in the winter (Fig. 7c).

Soil temperatures at 0.05 m estimated at the end of April and beginning of May (Fig. 7j) showed greater oscillation than those measured by the sensors, since a constant temperature had been assumed at 0.5 m. During this period, solar radiation was similar over the 5 days, but maximum wind speed at noon fell from 4 to 2.5 m s^{-1} (Fig. 5b), and consequently the air temperature inside the greenhouse raised from 25 to 30 ºC, increasing the heat transfer in the soil and the soil temperature at 0.05 m depth.

The model developed in the present work included the computation of ventilation rate G considering different discharge coefficients for roof C_{dVR} and side openings C_{dVS}. Most greenhouse temperature prediction models use the same coefficient C_d for side and roof openings (Baptista et al., 2010; Fatnassi et al., 2013; Mashonjowa et al., 2013). In the same way, we have considered different wind effect coefficients C_w for Northeast or Southwest winds, using a linear regression of the wind direction angle f_G as correction function for G. The use of this function f_G allowed correction of the ventilation flux G (Fig. 8a) and an improved estimation of T_i (Fig. 8b), reducing the RMSE by 0.05 ºC and RMSPE by 0.38%.

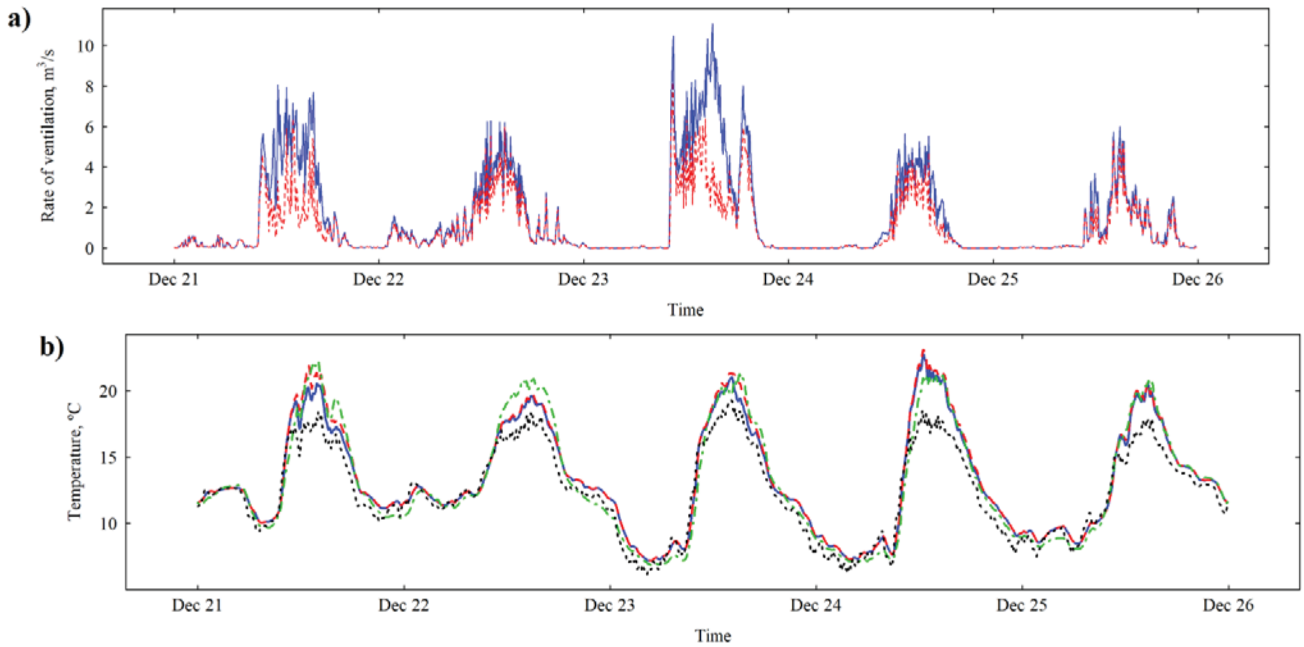

Fig. 8. Evolution of the ventilation flux G (——) calculated with Eq. (29) and corrected with the wind direction factor $f_G \cdot G$ (- - -) defined by Eq. (30) (a). Comparison of inside temperatures T_i (G) (——) computed using the ventilation flux G calculated with Eq. (29) and T_i (f_G, G) (- - -) estimated including the wind direction correction factor f_G with the measured inside (-·-·-) and outside (····) temperatures (b).

In warm or hot climatic conditions, the influence of heat flux exchanged by ventilation becomes fundamental in the energy balance of the greenhouse, with a decisive bearing on the estimation of air temperature. For this reason, the computation of this heat flux is more important than in cold areas where the quantity of air exchanged by ventilation and the outside-inside difference of temperature are lower. The developed model should be used in warm climates where strong inside-outside temperature gradients occur at noon in spring and summer.

There is no fixed criterion to determine that the accuracy of a simulation model is satisfactory, and consequently to consider it validated. Vanthoor et al. (2011a) consider that for the design of climate control systems a value of RMSPE lower or equal to 10% can be considered acceptable. However, the accuracy of a simulation model is conditioned by the thermal amplitude (difference between minimum and maximum outside temperatures), the heterogeneity of the temperature distribution inside the greenhouse (difference between hottest and coldest points) and the time period analysed.

The greater the thermal amplitude, the more difficult the estimation of inside temperature is. In the same way, the longer the period analysed, the higher the variability in parameters used as primary boundary conditions (solar radiation and wind patterns) and in greenhouse characteristics included in the model (transmissivity of the greenhouse cover and crop development). Therefore, a model validated with lower thermal amplitudes and shorter time periods should obtain greater accuracy than one validated with more heterogeneous climatic conditions over longer periods.

The accuracy of the models reported in the bibliography varies considerably. Thus, the model *InverSim* validated for a 12-day period with a thermal amplitude of T_i=3-52ºC (Bouzo et al., 2006) obtained lower accuracy ($RMSE$=3.9 °C; R^2=0.88) than models validated with lower thermal amplitudes and time intervals, such as the models used by Lammari et al. (2012) and Hasni et al. (2011) with climatic data for a period of a week in France, obtaining $RMSE$=1.05 °C (T_i=14-27 ºC) and mean absolute error MAE=1.24 ºC (T_i=15-32 ºC). Other models, such as *MICGREEN* (Singh et al., 2006), were validated using only one day of measurements (T_i=14-28 ºC), obtaining values of $RMSE$=5.69 ºC for inside air, $RMSE$=3.21 ºC for soil surface temperature, $RMSE$=3.91 ºC for cover temperature and $RMSE$=3.70 ºC for canopy temperature. Similar values were obtained with the *SIMICROC* model (Briceño-Medina et al., 2011), validated using data recorded over three days (T_i=14-28ºC) with $RMSE$=4.22 ºC for inside air, *RMSE*=4.84 ºC for soil temperature, *RMSE*=3.99 ºC for cover temperature and *RMSE*=4.39 ºC for canopy temperature.

In this work, the greenhouse model was validated using 25 non-successive days with outside temperatures ranging from 4 to 33 ºC, and inside temperatures from 6.3 ºC to 36.9 ºC (Table 3), with differences inside the greenhouse reaching 8 ºC (Fig. 9a), on both cloudy and windy days (Fig. 9b), thus allowing the deficiencies of the model to be observed, with a view to improving it in the future. The differences between measured and estimated temperatures for the four components analysed were between *RMSE*=1.1 ºC for the inside temperature and *RMSE*=2.8 ºC for soil mulch (Table 5). However, the objective of the model is not to predict the temperature inside a greenhouse in infrequent or unusual conditions with absolute precision. The developed model could be used in the future as a design tool, analysing the effect of changes in the ventilation area, the characteristics of the soil mulch or the level of whitening.

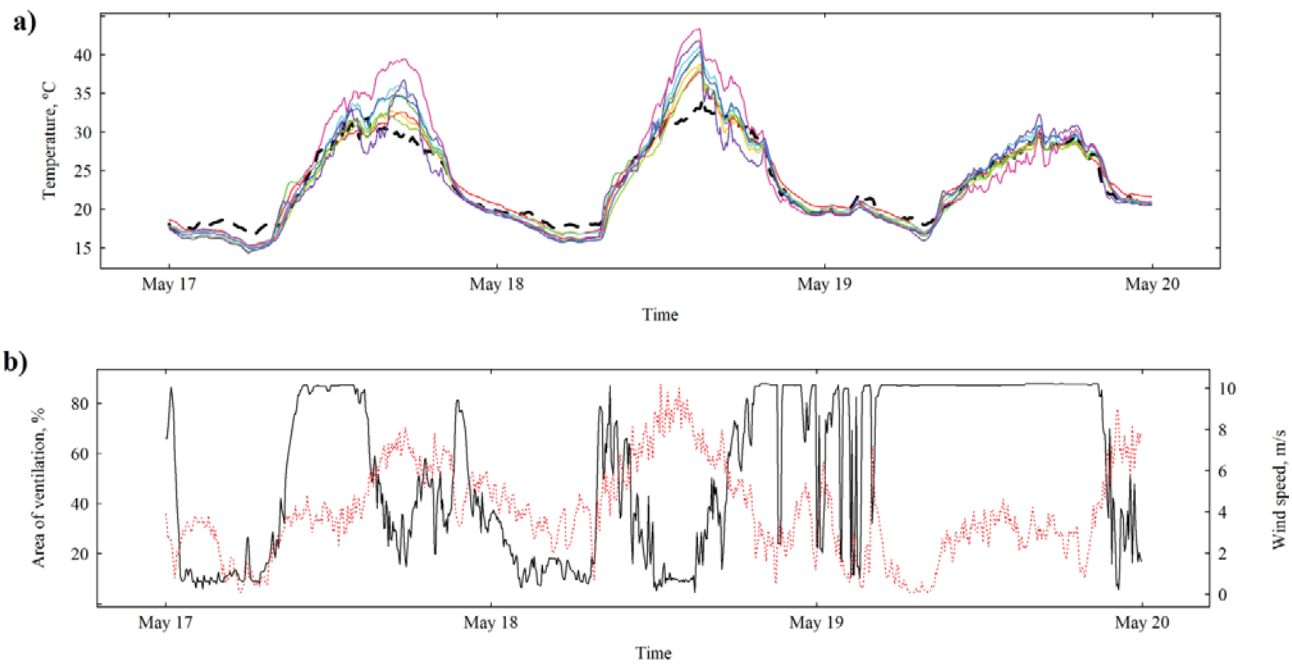

Fig. 9. Comparison on three spring days with similar outside temperatures between inside air temperatures T_i calculated (□□□□) and measured at different location-heights (Fig. 2): North-6 m (—), North-1 m (—), centre-1 m (—), South-1 m (—), North-2 m (—), centre-2 m (—), South-2 m (—), South-6 m (—) (a). Evolution over the three days (17-20 May 2015) of outside wind speed U_0 (- - -) and the ventilation opening percentage $(S_{VR}+S_{VS})/(S_{VRmax}+S_{VSmax})$ (—) (b).

3.2. Model limitations

Some discrepancies between measured and calculated values of T_i were observed on winter nights (Figs. 6a-b) and at noon in spring (Figs. 6d-e). These discrepancies could be attributed to various factors including: variations in heat storage in the soil on cold nights, variation in the heat flux exchanged by ventilation produced by differences between calculated inside temperature and temperature of air exiting the greenhouse (Molina-Aiz et al., 2012), and variations in the wind effect coefficient C_w depending on the wind and effect of turbulence on ventilation (Molina-Aiz et al., 2009). The maximum absolute difference in inside temperature of air between calculated and measured values was 4.3ºC at noon on May 3 when the inside temperature reached 31.8ºC, coinciding with rapid closure of the greenhouse openings as the climate control system responded to a strong wind in order to avoid structural damage.

The model underestimated the inside temperature on cold nights when a warm wind began to blow, rapidly increasing the outside temperature (Figs. 6a-b), producing thermal inversion (higher temperature outside than inside the greenhouse). Similar discrepancies were observed by Baptista et al. (2010) after opening or closing the vents, and approximately 2 h were required to the model to readjust. Without solar radiation, the model is affected by sudden changes in outside temperature and during the day by changes in ventilation, both produced by the oscillation of wind conditions, which is characteristic of the province of Almería. Hasni et al. (2011) and Fatnassi et al. (2013) also observed greater discrepancies between the model and measurements at night, with calculated air temperatures about 1ºC greater than measured ones, as occurred on 5th January in our work (Fig. 6a). Mashonjowa et al. (2013) also observed most of the significant differences between measured and calculated ventilation rates during the night.

When the weather changes drastically, as for example on 22nd December and 15th April when solar radiation suddenly fell (Fig. 5a), simulated temperatures differ considerably from measured values (Figs. 6a & 6c). The lower calculated inside air temperature is produced by the consideration of a constant value of solar transmittance τ_{cw}=0.42 of the greenhouse cover for all days of each period (Table 4). On cloudy days such as 15th April, measured global radiation inside and outside were very similar (Fig. 5a), because the real transmittance of the whitened cover approached a value of τ_{cw}=0.9 due to the diffusive characteristics of the light entering the greenhouse. To improve accuracy of the model on cloudy days, different transmittance coefficients could be considered for direct and diffuse light. However, commercial greenhouses only measure the global solar radiation, therefore this modification could reduce the simplicity of the model, which is one of the objectives of the present work.

The difficulty to model the greenhouse microclimate was observed on 7th to 9th January, with similar solar radiation (Fig. 5a) and wind (Fig. 5b) conditions resulting in similar maximum air temperatures at noon that the model is not capable of predicting (Fig. 6b). The model predicted a lower air temperature because of the greater wind speed recorded on 9th January. In this period, we can also observe the influence of wind direction, because on 7th January, solar radiation and wind speed were similar to the three following days of the period, but with a *Poniente* wind blowing from the Southwest instead of the *Levante* wind blowing from the Northeast (Fig. 5b). Although, wind direction significantly affects the ventilation rate and the air and crop temperature distributions in multispan greenhouses (Teitel et al., 2008), most simulation models neglect this influence on the energy balance.

Greater errors in the estimation of inside air temperature occurred at higher wind speeds, showing the importance of the ventilation flux in the energy balances inside the greenhouse (Fig. 9). A technical disadvantage of the multispan greenhouses in windy and hot climatic conditions is the need to close the vent openings at wind speeds over 8 m s^{-1} (28.8 km h^{-1}). Faced with strong winds, the control system begins to close the greenhouse openings progressively when wind speed surpasses 6 m s^{-1} (Fig. 9b) to avoid storm damage, and the openings stay closed until the wind diminishes. Under such conditions, the temperature rises inside the greenhouse as a result of the reduction of air exchange with the cooler outside air. A second consequence of the reduction in air movement is the stagnation of inside air, which can be observed by an increase in the heterogeneity in the temperature distribution (Fig. 9a). The temperature of air stagnated near the greenhouse cover (at 6 m height) can increase by about 7-8 ºC with respect to the plant zone (at 1 m height). This heterogeneity of air temperature produces an inaccuracy of the model, which assumes that the temperature of air exiting the greenhouse via the roof openings is equal to the average inside air temperature. The errors in estimation of inside air temperature increased with wind speed (Fig. 10). Differences between measured and calculated inside air temperatures $|T_{iM} - T_{iC}|$ of over 4 ºC were observed for both *Poniente* and *Levante* winds of over 6 m s^{-1} (Fig. 10). When the air velocity fell (Fig. 9b), the temperature uniformity was rapidly re-established inside the greenhouse and the simulated temperatures agreed with the measured values at different points inside the greenhouse (Fig. 9a).

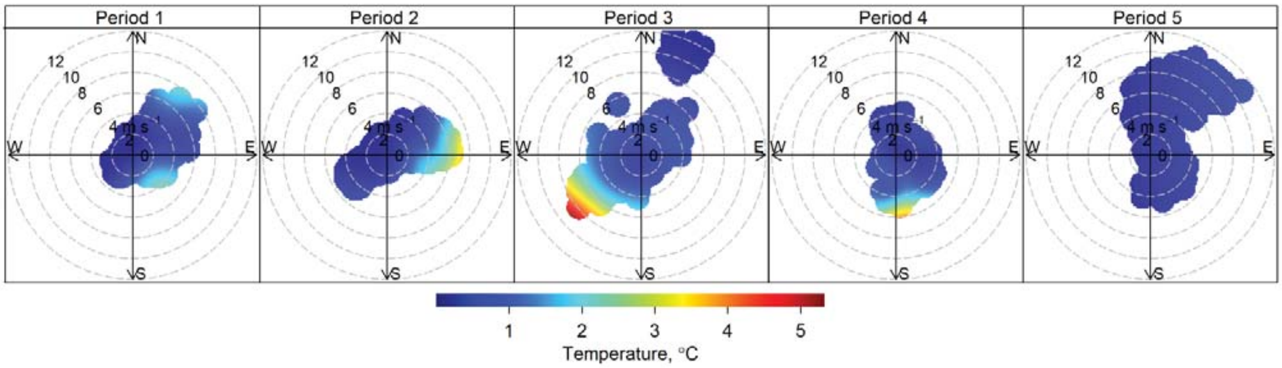

Fig. 10. Absolute differences between measured and calculated inside air temperatures $|T_{iM} - T_{iC}|$ as a function of wind speed U_0 and direction θ_w during five time periods: 21-25 December 2014 (Period 1), 5-9 January 2015 (Period 2), 15-19 April 2015 (Period 3), 29 April– 3 May 2015 (Period 4) and 1-5 June 2015 (Period 5).

The assumption of air temperature uniformity inside the greenhouse is the mayor drawback of energy balance models applied to naturally ventilated greenhouse in warm climates. In greenhouses with artificial climatic systems, whether heating (hot water pipes) or cooling (fog systems), the air temperature distribution inside remains more or less constant while the system works, making it easy to model the air temperature. In these conditions, the interior temperature depends to a great extent on the heat supplied or removed artificially, which is well-known, and therefore accurate estimations are obtained. Consequently, inaccurate estimation of the air exchanged by ventilation and the differences between air exiting the greenhouse and the average value inside the greenhouse constitute two major limitations of the model developed in this work, and in general, of all simulation models. Computational Fluid Dynamics (CFD) models present the advantage of taking into account temperature distributions inside the greenhouses, and could help to improve dynamic models using a thermal eefficiency coefficient η_T (Molina-Aiz and Valera, 2011) to calculate the heat exchanged by ventilation (Molina-Aiz et al., 2012).

Conclusions

The dynamic model developed in this work, based on six energy balance differential equations coupled with an empirical linear regression (Wang and Deltour, 1999), allows us to estimate the evolution over time of air, greenhouse cover, polypropylene mulch and soil temperatures with acceptable accuracy ($RMSE$=1.1-2.8 ºC).

Greater errors were produced in the estimation of inside air temperature at higher wind speeds, which highlights the importance of the ventilation flux in the energy balances inside the greenhouse. The model improved thanks to the use of different variable discharge coefficients for roof C_{dVR} and side openings C_{dVS}, different wind effect coefficients C_w for Northeast or Southwest winds, and a linear regression of the wind direction as a correction function of the volumetric ventilation flux G.

The main differences between measured and calculated values for inside temperature were observed on cloudy and windy days. On cloudy days, the change in the fraction of diffuse radiation produced the variation in the cover transmissivity, considered constant for each period in the model. On windy days, the climate control system closed the vent openings up to a point to prevent structural damage, thereby increasing heterogeneity of the inside air temperature. Under such circumstances, the temperature of air exiting the greenhouse via the openings was at a different temperature to the average inside air, invalidating the assumption of temperature uniformity.

A major problem that occurs in multispan greenhouses in areas such as Almería is the closure of vent openings when wind speed surpasses 8 m s^{-1} to avoid structural damage. The reduction of air movement inside the greenhouse produces considerable heterogeneity in temperature distribution, with differences in temperature of about 7-8 ºC between the warm zones near the crop (cooling air by evapotranspiration) and very hot areas near the greenhouse cover in the middle of spans (where hot air accumulates due to the buoyancy effect).

Acknowledgements

This research has been funded by the National R+D+i Plan Project AGL2015-68050-R of the Spanish Ministry of Economy and Competitiveness and ERDF funds.

References

Abdel-Ghany, A.M., Al-Helal, I.M., 2011. Solar energy utilization by a greenhouse: General relations. Renewable Energy. 36 (1), 189–196. https://doi.org/10.1016/j.renene.2010.06.020

Abdel-Ghany, A.M., Kozai, T., 2006. Dynamic modeling of the environment in a naturally ventilated, fog-cooled greenhouse. Renewable Energy. 31 (10), 1521–1539. http://doi.org/10.1016/j.renene.2005.07.013

Abdel-Ghany, A.M., Ishigami, Y., Goto, E., Kozai, T., 2006. A method for measuring greenhouse cover temperature using a thermocouple. Biosystems Engineering. 95 (1), 99–109. http://doi.org/10.1016/j.biosystemseng.2006.05.014

Abu-Hamdeh, N.H., Reeder, R.C., 2000. Soil thermal conductivity: effects of density, moisture, salt concentration, and organic matter. Soil Science Society of America Journal. 64, 1285–1290. http://doi.org/10.2136/sssaj2000.6441285x

Andersen, L., Kühn, B.F., Bertelsen, M., Bruus, M., Larsen, S.E., Strandberg, M., 2013. Alternatives to herbicides in an apple orchard, effects on yield, earthworms and plant diversity. Agriculture, Ecosystems & Environment. 172 (1), 1–5. http://doi.org/10.1016/j.agee.2013.04.004

Arbel, A., Shklyar, A., Barak, M., 2000. Buoyancy-driven ventilation in a greenhouse cooled by a fogging system. Acta Horticulturae. 534, 327–334. http://doi.org/10.17660/ActaHortic.2000.534.38

Bailey, B., Montero, J., Parra, J.P., Robertson, A., Baeza, E., Kamaruddin, R., 2003. Airflow resistance of greenhouse ventilators with and without insect screens. Biosystems Engineering. 86 (2), 217–229. https://doi.org/10.1016/S1537-5110(03)00115-6

Baille, A., Kittas, C., Katsoulas, N., 2001. Influence of whitening on greenhouse microclimate and crop energy partitioning. Agricultural and Forest Meteorology. 107 (4), 293–306. https://doi.org/10.1016/S0168-1923(01)00216-7

Baptista, F., Bailey, B.J., Meneses, J.F., Navas, L.M., 2010. Greenhouses climate modelling. Tests, adaptation and validation of a dynamic climate model. Spanish Journal of Agricultural Research. 8, 285–298. http://doi.org/10.5424/sjar/2010082-1629

Blasco, X., Martínez, M., Herrero, J.M., Ramos, C., Sanchis, J., 2007. Model-based predictive control of greenhouse climate for reducing energy and water consumption. Computer and Electronic in Agriculture. 55

(1), 49–70. http://doi.org/10.1016/j.compag.2006.12.001

Bot, G.P.A., 1980. Validation of a dynamical model of greenhouse climate. Acta Horticulturae. 106, 149–158. http://dx.doi.org/10.17660/ActaHortic.1980.106.19

Bot, G.P.A., 1989a. Greenhouse simulation models. Acta Horticulturae. 245, 315–325. http://dx.doi.org/10.17660/ActaHortic.1989.245.42

Bot, G.P.A., 1989b. A validated physical model of greenhouse climate. Acta Horticulturae. 245, 389–396. http://dx.doi.org/10.17660/ActaHortic.1989.245.52

Boulard, T., Baille, A., 1987. Analysis of thermal performance of a greenhouse as a solar collector. Energy in Agriculture. 6 (1), 17–26. http://dx.doi.org/10.1016/0167-5826(87)90018-0

Boulard, T., Baille, A., 1993. A simple greenhouse climate control incorporating effects of ventilation and evaporative cooling. Agricultural and Forest Meteorology. 65 (3), 145-157. http://dx.doi.org/10.1016/0168-1923(93)90001-X

Boulard, T., Draoui, B., Neirac, F., 1996. Calibration and validation of a greenhouse climate control model. Acta Horticulturae. 406, 49–62. https://doi.org/10.17660/ActaHortic.1996.406.4

Bouzo, C., Gariglio. N., Pilatti. R., Grenón. D., Favaro. J., Bouchet. F., Freyre. C., 2006. 'INVERSIM': a simulation model for a greenhouse. Acta Horticulturae. 719, 271–279. https://doi.org/10.17660/ActaHortic.2006.719.30

Briceño-Medina, L.Y., Ávila-Marroquín, M., Jaimez-Arellano, R., 2011. SIMICROC: modelo de simulación del microclima de un invernadero. Agrociencia. 45 (7), 801–813. (in Spanish with English abstract) < http://www.scielo.org.mx/pdf/agro/v45n7/v45n7a6.pdf>

Brzustowski, T.A. and Sommer, E.C. (1973). Predicting radiant heating from flares. Proceding of Division of Refining, American Petroleum Institute (API). 53, 865–893.

CAPDR, 2016. Cartografía de invernaderos en el litoral de Andalucía Oriental. Año 2016. (Cartography of greenhouses in the Eastern Andalusian Coast. Year 2016). Consejería de Agricultura Pesca y Desarrollo Rural (CAPDR). Junta de Andalucía, Andalucía (España), 20 pp. (In Spanish) <http://www.juntadeandalucia.es/export/drupaljda/estudios_informes/16/12/Cartografia%20invernaderos%20en%20el%20litoral%20de%20Andaluc%C3%ADa%20Oriental_v161201.pdf>

Castañeda-Miranda, A., Castaño, V.M., 2017. Smart frost control in greenhouses by neural networks models. Computers and Electronics in Agriculture. 137, 102–114. https://doi.org/10.1016/j.compag.2017.03.024.

de Halleux, D., Deltour, J., Nijskens, J., Nisen, A., Coutisse, S., 1985. Dynamic simulation of heat fluxes and temperatures in horticultural and low emissivity glass-covered greenhouses. Acta Horticulturae. 170, 91–96. https://doi.org/10.17660/ActaHortic.1985.170.9

Deltour, J., de Halleux, D., Nijskens, J., Coutisse, S., Nisen, A., 1985. Dynamic modelling of heat and mass transfer in greenhouses. Acta Horticulturae. 174, 119–125. https://doi.org/10.17660/ActaHortic.1985.174.14

Donatelli, M., Bellocchi, G., Carlini, L., 2006. Sharing knowledge via software components: Models on reference evapotranspiration. Eururopena Journal of Agronomy. 24 (2), 186–192. http://dx.doi.org/10.1016/j.eja.2005.07.005

Duarte-Galván, C., Torres-Pacheco, I., Guevara-Gonzalez, R., Romero-Troncoso, R., Contreras-Medina, L., Rios-Alcaraz, M., Millan-Almaraz, J., 2012. Advantages and disadvantages of control theories applied in greenhouse climate control systems. Spanish Journal of Agricultural Research. 10, 926–938. http://dx.doi.org/10.5424/sjar/2012104-487-11

Espinoza, K., Valera, D.L., Torres, J.A., López, A., Molina-Aiz, F.D., 2015. An auto-tuning PI control system for an open-circuit low-speed wind tunnel designed for greenhouse technology. Sensors. 15 (8), 19723–19749. http://dx.doi.org/10.3390/s150819723

Farina, E., Allera, C., Paterniani, T., Palagi, M., 2003. Mulching as a technique to reduce salt accumulation in soilless culture. Acta Horticulturae. 609 (1), 459-466. https://doi.org/10.17660/ActaHortic.2003.609.71

Fatnassi, H., Boulard, T., Bouirden, L., 2013. Development, validation and use of a dynamic model for simulate the climate conditions in a large scale greenhouse equipped with insect-proof nets. Compututers and Electronics in Agriculture. 98, 54–61. https://doi.org/10.1016/j.compag.2013.07.008

Feuilloley, P., Guillaume, S., Issanchou, G., Davenel, A., 1990. Determination of thermal transparency of plastics material for covering greenhouses. Acta Horticulturae. 281, 57-66. http://dx.doi.org/10.17660/ActaHortic.1990.281.5

Fitz-Rodríguez, E., Kubota, C., Giacomelli, G.A., Tignor, M.E., Wilson, S.B., McMahon, M., 2010. Dynamic modeling and simulation of greenhouse environments under several scenarios: A web-based application.

Computers and Electronics in Agriculture. 70 (1): 105–116. http://doi.org/10.1016/j.compag.2009.09.010.

FranceAgriMer, 2013. Rapport évaluation ex post des programmes de financement de certaines dépenses de modernisation dans le secteur des serres maraichères et horticoles. Unité Evaluation FranceAgriMer. Étabalissement National des Produits de l'Agriculture et de la Mer. 224 pp. http://www.franceagrimer.fr/content/download/29759/264211/file/%C3%A9valuationaidesserres.pdf

Ganguly, A., Ghosh, S., 2009. Model development and experimental validation of a floriculture greenhouse under natural ventilation. Energy and Buildings. 41 (5), 521–527. https://doi.org/10.1016/j.enbuild.2008.11.021

Garzoli, K.V., Blackwell, J., 1981. An analysis of the nocturnal heat loss from a single skin plastic greenhouse, Journal of Agricultural Engineering Research. 26 (3), 203–214. http://dx.doi.org/10.1016/0021-8634(81)90105-0

Garzoli, K., 1985. A simple greenhouse climate model. Acta Horticulturae. 174, 393–400. https://doi.org/10.17660/ActaHortic.1985.174.52

Goudriaan, J., 1977. Crop micrometeorology: a simulation study. Simulation Monographs. Centre for Agricultural Publishing and Documentation (PUDOC), Wageningen, The Netherlands, 249 pp. <http://library.wur.nl/WebQuery/clc/104086>

Hasni, A., Taibi, R., Draoui, B., Boulard, T., 2011. Optimization of Greenhouse Climate Model Parameters Using Particle Swarm Optimization and Genetic Algorithms. Energy Procedia. 6, 371–380. http://dx.doi.org/10.1016/j.egypro.2011.05.043

Hamdhan, I.N. and Clarke, B.G. (2010). Determination of thermal conductivity of coarse and fine sand soils. Proceedings World Geothermal Congress 2010. 25-29 April 2010, Bali (Indonesia), 7 pp. <https://www.geothermal-energy.org/pdf/IGAstandard/WGC/2010/2952.pdf>

He, F., Ma, C., 2010. Modeling greenhouse air humidity by means of artificial neural network and principal component analysis. Computers and Electronics in Agriculture. 71 (Supplement 1), S19–S23. https://doi.org/10.1016/j.compag.2009.07.011

Hyndman, R.J., Koehler, A.B., 2006. Another look at measures of forecast accuracy. International Journal of Forecasting, 22(4), 679–688. http://dx.doi.org/10.1016/j.ijforecast.2006.03.001

Iziomon, M.G., Mayer, H., Matzarakis, A., 2003. Downward atmospheric longwave irradiance under clear and cloudy skies: Measurement and parameterization. Journal of Atmospheric and Solar-Terrestrial Physics. 65 (10), 1107–1116. http://doi.org/10.1016/j.jastp.2003.07.007

Joudi, K.A., Farhan, A.A., 2015. A dynamic model and an experimental study for the internal air and soil temperatures in an innovative greenhouse. Energy Conversion and Management. 91, 76–82. https://doi.org/10.1016/j.enconman.2014.11.052

Kang, Y., Chang, Y.C.A., Choi, H.S., Gu, M., 2013. Current and future status of protected cultivation techniques in Asia. Acta Horticulturae. 987, 33–40. https://doi.org/10.17660/ActaHortic.2013.987.3

Kano, A., Sadler, E.J., 1985. Survey of greenhouse models. Journal of Agricultural Meteorology. 41 (1), 75–81. http://doi.org/10.2480/agrmet.41.75

Kimball, B.A. 1973. Simulation of the energy balance of a greenhouse. Agricultural Meteorology. 11, 243–260. http://dx.doi.org/10.1016/0002-1571(73)90067-8.

Kindelan, M., 1980. Dynamic Modeling of Greenhouse Environment. Transactions of the ASAE. 23 (5), 1232–1239. http://dx.doi.org/10.13031/2013.34752

Kittas, C., 1986. Greenhouse cover conductances. Boundary-Layer Meteorology. 36, 213–225. http://dx.doi.org/10.1007/BF00118660

Kittas, C., Boulard, T., Papadakis, G., 1997. Natural ventilation of a greenhouse with ridge and side openings: sensitivity to temperature and wind effects. Transactions of the ASAE. 40 (2), 415–425. http://dx.doi.org/10.13031/2013.21268

Kobayashi, K., Salam, M.U., 2000. Comparing simulated and measured values using mean squared deviation and its components. Agronomy Journal. 92(2), 345–352. http://dx.doi.org/10.2134/agronj2000.922345x

Kottegoda, N.T., Rosso, R., 2008. Applied statistics for civil and environmental engineers. 2nd Edition. Blackwell Publishing Ltd. Oxford, United Kingdom, 718 pp.

Krauss G., Depecker, P., Kindagen, J.I., 1997. Méthode des réseaux de neurones pour le calcul des coefficients de vitesse. Application aux écoulements de l'air dans les bâtiments. Revue Génerale de Thermique. 36 (3), 180-191. https://doi.org/10.1016/S0035-3159(97)88158-5 (in French with English abstract)

Kuciauskas, A.P., Brody, L.R., Hadjimichael, M., Bankert, R.L., Tag, P.M., Peak, J.E., 1998. A fuzzy expert system to assist in the prediction of hazardous wind conditions within the Mediterranean basin.

Meteorological Applications. 5 (4), 307–320. https://doi.org/10.1017/S1350482798001005

Kumar, K.S., Jha Madan, K., Tiwari, K.N., 2010. Modeling and evaluation of greenhouse for floriculture in subtropics. Energy and Buildings. 42 (7), 1075–1083. https://doi.org/10.1016/j.enbuild.2010.01.021

Kurzböck, M., Wallner, G.M., Lang, R.W., 2012. Black pigmented polypropylene materials for solar absorbers. Energy Procedia. 30, 438–445. https://doi.org/10.1016/j.egypro.2012.11.052

Lafont, F., Balmat, J.F., Pessel., N., Fliess, M., 2015. A model-free control strategy for an experimental greenhouse with an application to fault accommodation. Computers and Electronics in Agriculture. 110, 139–149. http://doi.org/10.1016/j.compag.2014.11.008

Lammari, K., Bounaama, F., Draoui, B., Mrah, B., Haidas, M., 2012. GA optimization of the coupled climate model of an order two of a greenhouse. Energy Procedia. 18, 416–425, http://dx.doi.org/10.1016/j.egypro.2012.05.053

Linker, R., Seginer, I., 2004. Greenhouse temperature modeling: a comparison between sigmoid neural networks and hybrid models. Mathematics and Computers in Simulation. 65 (1–2), 19–29. https://doi.org/10.1016/j.matcom.2003.09.004

López, A., 2011. Contribución al conocimiento del microclima de los invernaderos mediterráneos mediante anemometrıía sónica y termografía (Contribution to the knowledge of Mediterranean greenhouse microclimate through sonic anemometry and thermography). PhD thesis, University of Almería, Almería, Spain, 512 pp. (in Spanish with English abstract)

López, A., Valera, D.L., Molina-Aiz, F.D., Peña, A., 2011. Effects of surrounding buildings on air patterns and turbulence in two naturally ventilated Mediterranean greenhouses using tri-sonic anemometry. Transactions of the ASABE. 54 (5), 1941–1950. http://dx.doi.org/10.13031/2013.39835

López, A., Molina-Aiz, F.D., Valera, D.L., Peña, A., 2016. Wind tunnel analysis of the airflow through insect-proof screens and comparison of their effect when installed in a Mediterranean greenhouse. Sensors. 16, 690. http://dx.doi.org/10.3390/s16050690

MAGRAMA, 2014.- Superficies y producciones anuales de cultivos. 2014. (Crops yearly area and yield. 2014). Ministerio de Agricultura, Alimentación y Medio Ambiente (MAGRAMA), Madrid (Spain), 357 pp. (In Spanish) <http://www.mapama.gob.es/estadistica/pags/anuario/2015/CAPITULO%20PDF/AE15-C13.pdf>

Mashonjowa, E., Ronsse, F., Milford, J.R., Pieters, J.G., 2013. Modelling the thermal performance of a naturally ventilated greenhouse in Zimbabwe using a dynamic greenhouse climate model. Solar Energy. 91, 381–393. http://dx.doi.org/10.1016/j.solener.2012.09.010

Mihara, Y., Hayashi, M., 1978. Latent heat of water for cooling and dehumidifying ventilation in greenhouses. Acta Horticulturae. 87, 329–336. https://doi.org/10.17660/ActaHortic.1978.87.35

Molina-Aiz, F.D., Valera, D.L., 2011. Optimization of almería-type greenhouse vent configuration by evaluating ventilation efficiency based on Computational Fluid Dynamics. Acta Horticulturae. 893, 669–677. https://doi.org/10.17660/ActaHortic.2011.893.71

Molina-Aiz, F.D., Valera D.L., López, A., Álvarez, A.J., 2012. Analysis of cooling ventilation efficiency in a naturally ventilated Almería-type greenhouse with insect screens. Acta Horticulturae. 927, 551-558. http://dx.doi.org/10.17660/ActaHortic.2012.927.67

Molina-Aiz, F.D., Valera, D.L., Peña, A.A., Gil, J.A., López, A., 2009. A study of natural ventilation in an Almería-type greenhouse with insect screens by means of tri-sonic anemometry. Biosystems Engineering. 104 (2), 224–242. https://doi.org/10.1016/j.biosystemseng.2009.06.013

Monteith, J.L., Unsworth, M.H., 2008. Principal of environmental physics. Plants, Animals, and the Atmosphere. 4th Ed. Academic Press-Elsevier, Amsterdam, The Netherlands, 401 pp. http://doi.org/10.1016/B978-0-12-386910-4.00008-1

Montgomery, R.B., 1947. Viscosity and thermal conductivity of air and diffusivity of water vapor in air. Journal of Atmospheric Sciences. 4 (6), 193–196. http://dx.doi.org/10.1175/1520-0469(1947)004<0193:VATCOA>2.0.CO;2

Nijskens, J., Deltour, J., Coutisse, S., Nisen, A., 1984. Heat transfer through covering materials of greenhouses. Agricultural and Forest Meteorology. 33 (2–3), 193-214. http://dx.doi.org/10.1016/0168-1923(84)90070-4

Nikiforova, T., Savytskyi, M., Limam, K., Bosschaerts, W., Belarbi, R., 2013. Methods and results of experimental researches of thermal conductivity of soils. Energy Procedia. 42, 775–783. http://dx.doi.org/10.1016/j.egypro.2013.12.034.

Nwoye, C.I., Nwakpa, S.O., Nwosu, I.E., Odo, J.U, Chinwuko, E.C. and Idenyi, N.E., 2014. Multi-factorial analysis of atmospheric noise pollution level based on emitted carbon and heat radiation during gas flaring.

Journal of Atmospheric Pollution. 2 (1), 22–29. http://dx.doi.org/10.12691/jap-2-1-5

Pardossi, A., Tognoni, F., Incrocci, L., 2004. Mediterranean greenhouse technology. Chronica Horticulturae. 44 (2), 28–34.

Pearson, C.C., Owen, J.E., 1994. The resistance to air flow of farm building ventilation components. Journal of Agricultural Engineering Research. 57 (1), 53–65. http://dx.doi.org/10.1006/jaer.1994.1005

Pieters, J., Deltour, J., Debruyckere, M., 1997. Condensation and dynamic heat transfer from greenhouses. Part I: theoretical model. Agricultural Engineering Journal, 5(3&4), 119–133.

Puszkarz, A.K., Korycki, R., Krucinskahttps, I., 2016. Simulations of heat transport phenomena in a three-dimensional model of knitted fabric. AUTEX Research Journal. 16 (3), 128 –137. http://dx.doi.org/10.1515/aut-2015-0042

Reyes-Rosas, A., Rodríguez-García, R., Zermeño-González, A., Jasso-Cantú, D., Cadena-Zapata, M., Burgueño-Camacho, H., 2012. Evaluation of a model for estimating the temperature and relative humidity Inside greenhouses with natural ventilation. Revista Chapingo. Serie horticultura. 18 (1), 125–140. < http://www.scielo.org.mx/pdf/rcsh/v18n1/v18n1a9.pdf>

Seginer, I., Boulard, T., Bailey, B.J., 1994. Neural network models of the greenhouse climate. Journal of Agricultural Engineering Research. 59 (3), 203–216. https://doi.org/10.1006/jaer.1994.1078

Seginer, I., 1997. Some artificial neural network applications to greenhouse environmental control. Computers and Electronics in Agriculture. 18 (2–3), 167–186. https://doi.org/10.1016/S0168-1699(97)00028-8

Sengar, S., Kothari, S., 2008. Thermal modeling and performance evaluation of arch shape greenhouse for nursery raising. African Journal of Mathematics and Computer Science Researc. 1 (1), 1–9. < http://www.academicjournals.org/article/article1379597037_Sengar and Kothari.pdf>

Sethi, V.P., Sumathy, K., Lee, C., Pal, D.S., 2013.Thermal modeling aspects of solar greenhouse microclimate control: A review on heating technologies. Solar Energy. 96, 56–82. https://doi.org/10.1016/j.solener.2013.06.034

Shcherbakov, M.V., Brebels, A., Shcherbakova, N.L., Tyukov, A.P., Janovsky, T.A., Kamaev, V.A., 2013. A survey of forecast error measures. World Applied Sciences Journal, 24, 171–176. DOI: 10.5829/idosi.wasj.2013.24.itmies.80032

Shklyar, A., Arbel, A., 2004. Numerical model of the three-dimensional isothermal flow patterns and mass fluxes in a pitched-roof greenhouse. Journal of Wind Engineering & Industrial Aerodynamics. 92, 1039–1059. https://doi.org/10.1016/j.jweia.2004.05.008

Singh, G., Singh, P.P., Singh-Lubana, P.P., Singh, K.G., 2006. Formulation and validation of a mathematical model of the microclimate of a greenhouse, Renewable Energy. 31 (10), 1541-1560. http://dx.doi.org/10.1016/j.renene.2005.07.011

Soetaert, K., Petzoldt, T. and Setzer, R.W. (2010). Solving differential equations in R: Package deSolve. Journal of Statistical Software. 33(9), 1–25. < https://journal.r-project.org/archive/2010-2/RJournal_2010-2_Soetaert~et~al.pdf>

Stanghellini, C., 1987. Transpiration of the greenhouse crop canopies: An aid to climate management. PhD thesis, Institute of Mechanisation, Labour and Buildings (IMAG), Wageningen, The Netherlands, 150 pp. <http://edepot.wur.nl/202121>

Sutherland, W., 1893. LII. The viscosity of gases and molecular force. Philosophical Magazine Series 5, 36 (223), 507-531. http://dx.doi.org/10.1080/14786449308620508

Swinbank, W.C., 1963. Long-wave radiation from clear skies. Quarterly Journal of the Royal Meteorological Society. 89 (381): 339–348. http://dx.doi.org/10.1002/qj.49708938105

Taki, M., Ajabshirchi, Y., Ranjbar, S.F., Rohani, A., Matloobi, M., 2016.- Heat transfer and MLP neural network models to predict inside environment variables and energy lost in a semi-solar greenhouse. Energy and Buildings. 110 (1), 314–329. https://doi.org/10.1016/j.enbuild.2015.11.010

Tchamitchian, M., Martin-Clouaire, R., Lagier, J., Jeannequin, B., Mercie,r S., 2006. SERRISTE: A daily set point determination software for glasshouse tomato production. Computers and Electronics in Agriculture. 50 (1), 25–47. https://doi.org/10.1016/j.compag.2005.07.004

Teitel, M., Ziskind, G., Liran, O., Dubovsky, V., Letan, R., 2008. Effect of wind direction on greenhouse ventilation rate, airflow patterns and temperature distributions. Biosystems Engineering. 101 (3), 351–369. http://doi.org/10.1016/j.biosystemseng.2008.09.004

Tüzel, Y., Öztekin, G.B., 2015. Protected cultivation in Turkey. Chronica Horticulturae. 55 (2), 21–26. http://www.ihc2018.org/files/downloads/Vol55-N02-Protected-cultivation-in-Turkey.pdf

Valera, D.L., Álvarez, A.J., Molina, F.D., 2006. Aerodynamic analysis of several insect-proof screens used in - greenhouses. Spanish Journal of Agricultural Research. 4 (4) 273–279. http://dx.doi.org/10.5424/sjar/2006044-204.

Valera, D., Belmonte, L., Molina-Aiz, F.D., López, A., 2016. Greenhouse agriculture in Almería. A comprehensive techno-economic analysis. Serie Economia. Cajamar Caja Rural, Spain. 408 pp. <http://www.publicacionescajamar.es/pdf/series-tematicas/economia/greenhouse-agriculture-in-almeria.pdf>

Vanthoor, B.H.E., Stanghellini, C., Van Henten, E.J., De Visser, P.H.B., 2011. A methodology for model-based greenhouse design: Part 1, a greenhouse climate model for a broad range of designs and climates. Biosystem Engineering. 110 (4), 363–377. http://doi.org/10.1016/j.biosystemseng.2011.06.001

Venables, W.N., Smith, D.M., (2016). An Introduction to R. Notes on R: A Programming Environment for Data Analysis and Graphics. Version 3.3.1. The R Core Team, 99 pp. <https://cran.r-project.org/>

Walker, J.N., 1965. Predicting temperatures in ventilated greenhouses. Transactions of the ASAE. 8 (3), 445–448. http://doi.org/10.13031/2013.40545

Wang, S., Boulard, T., 2000. Predicting the microclimate in a naturally ventilated plastic house in a Mediterranean climate. Journal of Agricultural Engineering Research. 75 (1), 27–38. https://doi.org/10.1006/jaer.1999.0482

Wang, S., Deltour, J., 1999. An experimental model for leaf temperature of greenhouse-grown tomato. Acta Horticulturae. 491, 101-106. https://doi.org/10.17660/ActaHortic.1999.491.13

Wypych, G., 2016. PP polypropylene. In: Handbook of Polymers. ChemTec Publishing. pp. 497–504. http://doi.org/10.1016/B978-1-895198-92-8.50156-7

Yang, N.W., Zang, L.S., Wang, S., Guo, J.Y., Xu, H.X., Zhang, F., Wan, F.H., 2014. Biological pest management by predators and parasitoids in the greenhouse vegetables in China. Biological Control. 68, 92–102. http://dx.doi.org/10.1016/j.biocontrol.2013.06.012

Yannas, S., Erell, E., Molina, J.L., 2006. Roof Cooling Techniques: A Design Handbook. Earthscan, London (UK), 164 p.

Zarandi, M.B., Bioki H.A., 2013. Thermal and mechanical properties of blends of LDPE and EVA crosslinked by electron beam radiation. European Physical Journal Applied Physic. 63, 21101.

https://doi.org/10.1051/epjap/2013130238

Appendix A. Discharge coefficient of the greenhouse openings

Discharge coefficient of vent opening can be estimated in function of a discharge coefficient characterising the shape of the openings C_{dHL} and a discharge coefficient $C_{d\varphi}$ corresponding to the effect of insect proof screens located in the openings (Arbel et al., 2000; Molina-Aiz et al., 2009):

$$C_{dj} = \sqrt{\frac{1}{\frac{1}{C_{dHLj}^{2}} + \frac{1}{C_{d\varphi}^{2}}}} \quad \text{(A.1)}$$

Discharge coefficient of an unscreened opening can been obtained from Bailey et al. (2003) as:

$$C_{dHLj} = \left[1.9 + 0.7\, exp\left(-L_{Vj}/(32.5 w_{Vj} sen\alpha_{Vj})\right)\right]^{-0.5} \quad \text{(A.2)}$$

where L_{Vj} is the length of the opening j (m), w_{Vj} is the height (m) and α_{Vj} is the angle of opening (with a value of α_{Vj}=90º for the side opening without flaps). For roof vents the maximum opening angle was α_{VR}=12.9º when were fully opened.

Heights of both side and roof openings w_{Vj} were reduced depending on the measured opening area by the climate control system, that opened or closed the windows according to the ventilation set up temperature fixed to 20 ºC during the season:

$$w_{VS} = \frac{S_{VS}}{L_{VS}} \quad \text{(A.3)} \qquad w_{VR} = \frac{S_{VR}}{L_{VR}} \quad \text{(A.4)}$$

The vent roof opening angle α_{vR} was calculated as:

$$\alpha_{VR} = arctg\left(\frac{w_{VR}}{4.2}\right) \quad \text{(A.5)}$$

The vertical distance between the midpoint of side and roof openings (Fig. 1a), used in Eq. (29), was also calculated at each time step in function of the opening level of both openings:

$$h_{SR} = 3.09 + w_{VR} + w_{VR} \quad \text{(A.6)}$$

The discharge coefficient of the insect proof screen $C_{d\varphi}$ can be obtained from the pressure loss coefficient F_{φ}:

$$C_{d\varphi} = \frac{1}{\sqrt{F_{\varphi}}} \quad \text{(A.7)}$$

Pressure loss coefficient can be calculated from the aerodynamic characteristic of the screen and the Reynold number as (Molina-Aiz et al., 2009):

$$F_{\varphi} = \frac{2e_{scr}}{K_p^{0.5}}\left(\frac{1}{Re_p} + Y\right) \qquad \text{(A.8)}$$

$$Re_p = \frac{K_p^{0.5}\rho_a v_V}{\mu_a} \qquad \text{(A.9)}$$

Permeability K_p (m^2) and inertial factor Y (Table 1) were obtained from wind tunnel tests (Valera et al., 2006; Espinoza et al., 2016) of a sample of the insect-proof screen installed in the greenhouse vents.

For the first time step (t=0 s) we used an initial value for air velocity through the greenhouse vents of v_V=0.2 m s^{-1} (Appendix B). For the following steps t_k we calculated an average air velocity from the value of volumetric airflow G at the preceding time step t_{k-1} computed with Eq. (29) as:

$$v_V(t_k) = \frac{2G(t_{k-1})}{S_{VS} + S_{VR}} \qquad \text{(A.10)}$$

Dynamic viscosity of air was calculated from simulated inside temperature using the following equation (Sutherland, 1893; Montgomery, 1947):

$$\mu_a = 1.4602x10^{-6}\frac{T_i^{3/2}}{T_i + 110} \qquad \text{(A.9)}$$

Density of inside air δ_a was calculated from temperature T_i and pressure (Donatelli et al., 2006):

$$\delta_a = \frac{P_e}{1.01R(T_i + 273.16)} \qquad \text{(A.10)}$$

where P_e is the pressure outside the greenhouse (Pa), considered equal to the atmospheric pressure at sea level, 101325 (Pa) and R is the specific gas constant, 287 (J kg^{-1}K^{-1}).

Appendix B. Computing Procedure

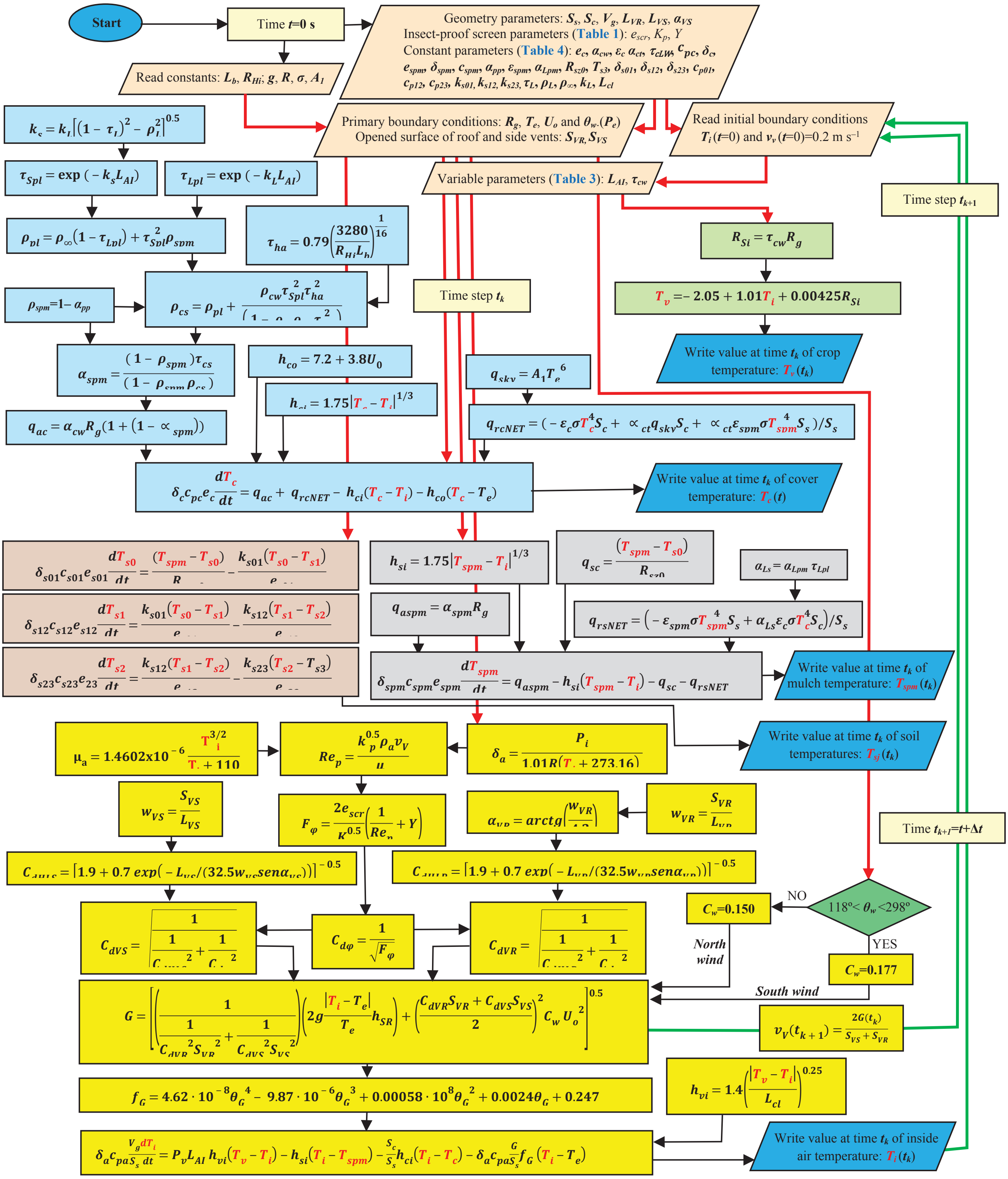

Fig. 11. Flowchart for computing greenhouse temperatures (for variable means and unit see nomenclature).

a)

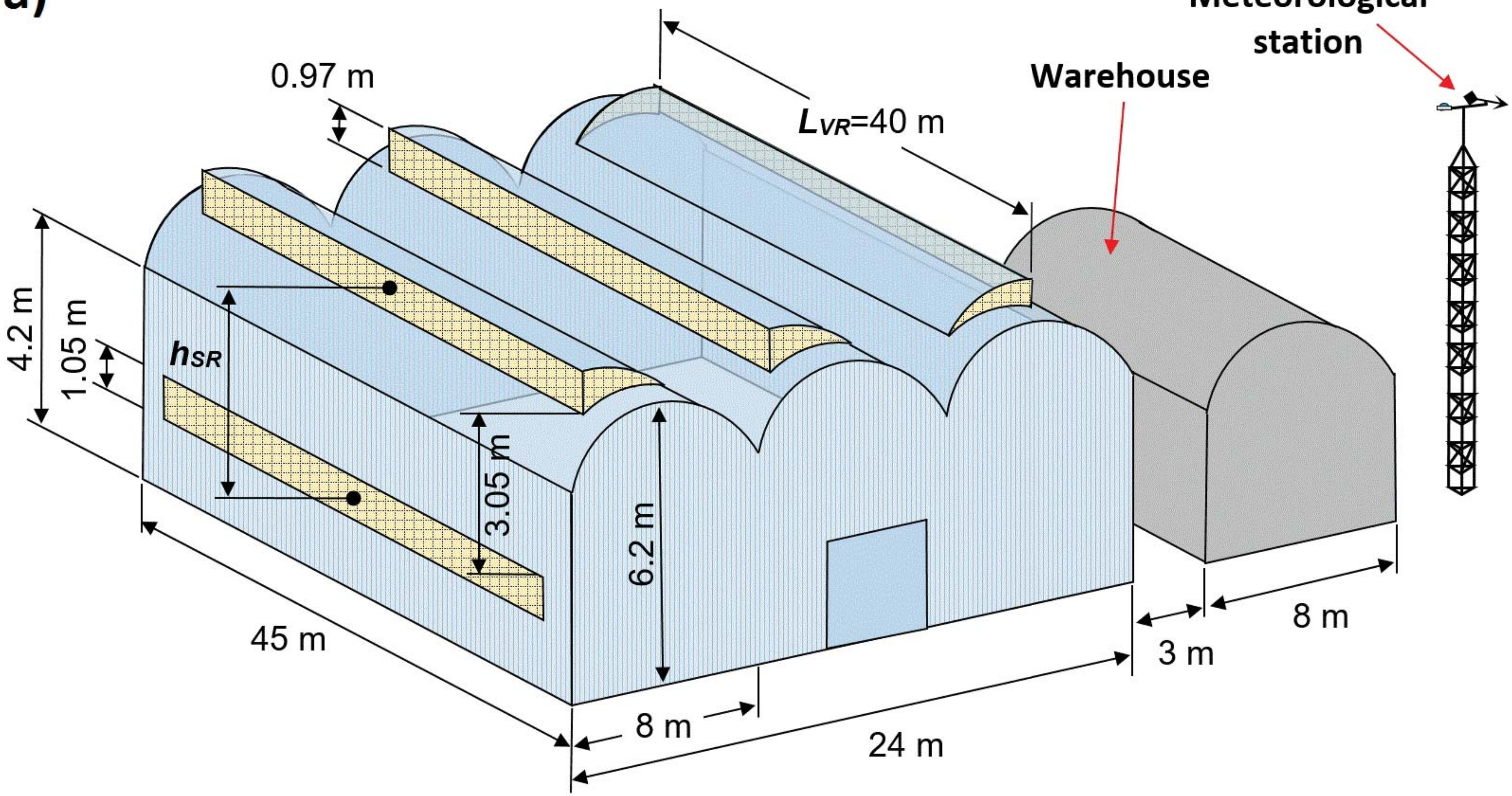

Meteorological station
Warehouse
0.97 m
L_{VR}=40 m
4.2 m
1.05 m
h_{SR}
3.05 m
6.2 m
45 m
8 m
24 m
3 m
8 m

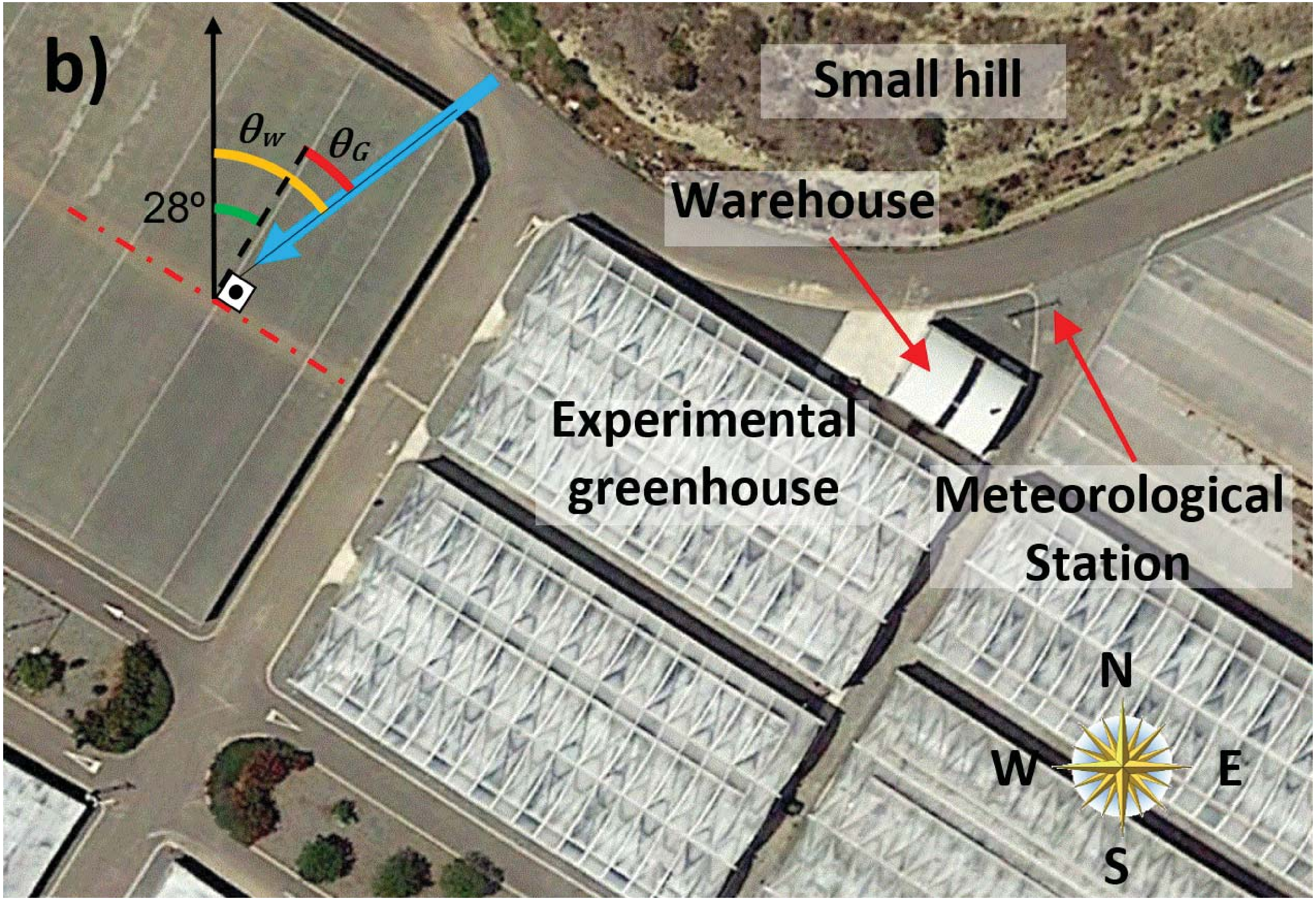
b)
Small hill
Warehouse
Experimental greenhouse
Meteorological Station
θ_W
θ_G
28º
N
W
E
S

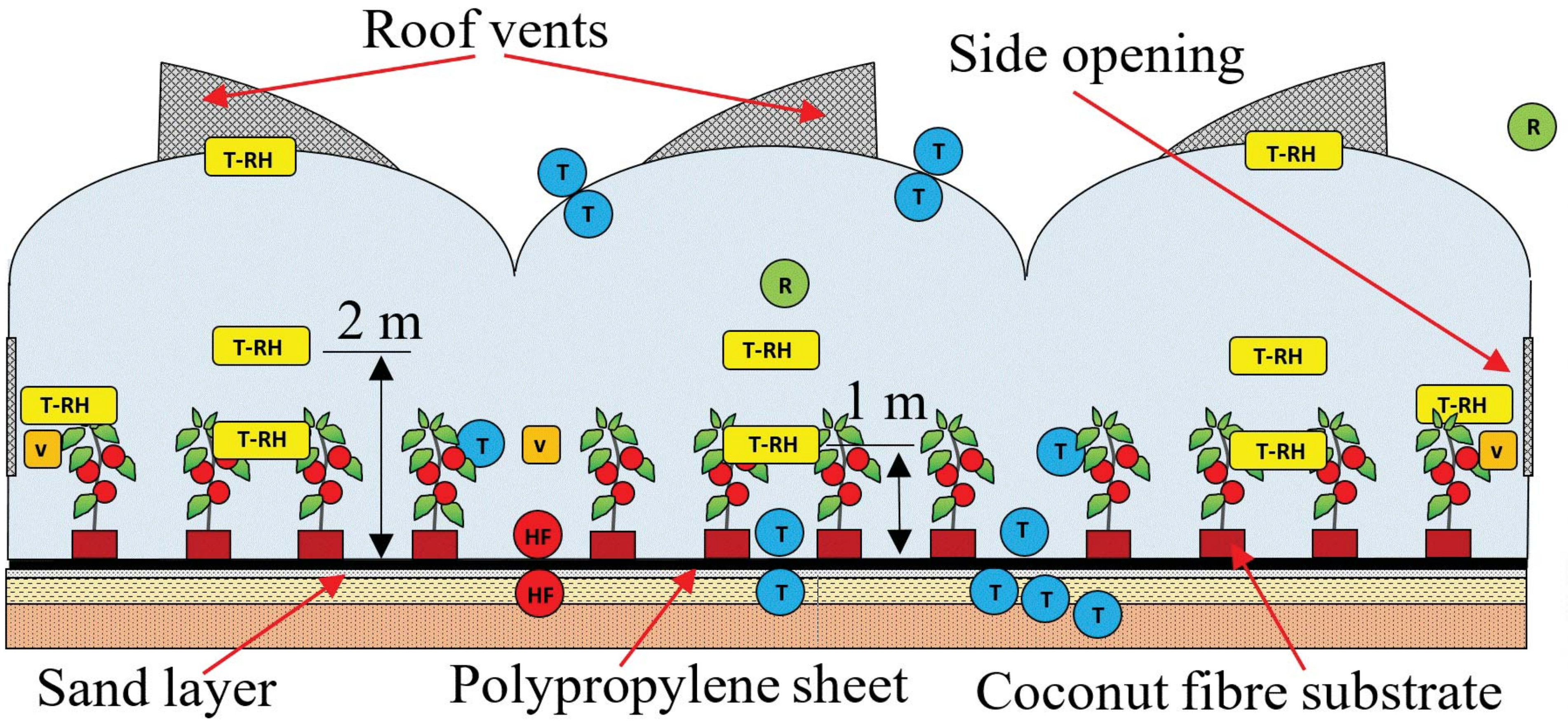
Roof vents
Side opening
2 m
1 m
T-RH
T
R
V
HF
Sand layer
Polypropylene sheet
Coconut fibre substrate

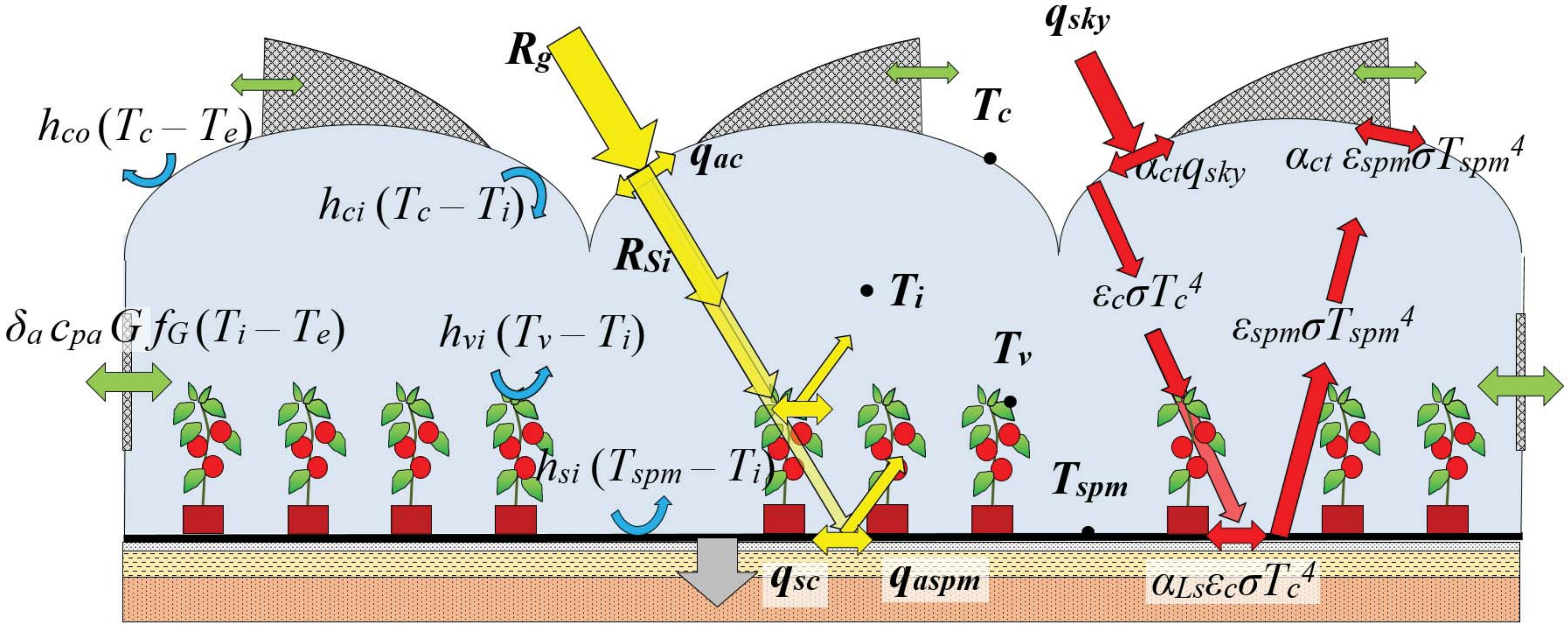

R_g
q_{sky}
T_c
$h_{co}(T_c - T_e)$
q_{ac}
$\alpha_{ct} q_{sky}$
$\alpha_{ct}\, \varepsilon_{spm} \sigma T_{spm}{}^4$
$h_{ci}(T_c - T_i)$
R_{Si}
T_i
$\varepsilon_c \sigma T_c{}^4$
$\delta_a c_{pa} G f_G (T_i - T_e)$
$h_{vi}(T_v - T_i)$
$\varepsilon_{spm} \sigma T_{spm}{}^4$
T_v
$h_{si}(T_{spm} - T_i)$
T_{spm}
q_{sc}
q_{aspm}
$\alpha_{Ls} \varepsilon_c \sigma T_c{}^4$

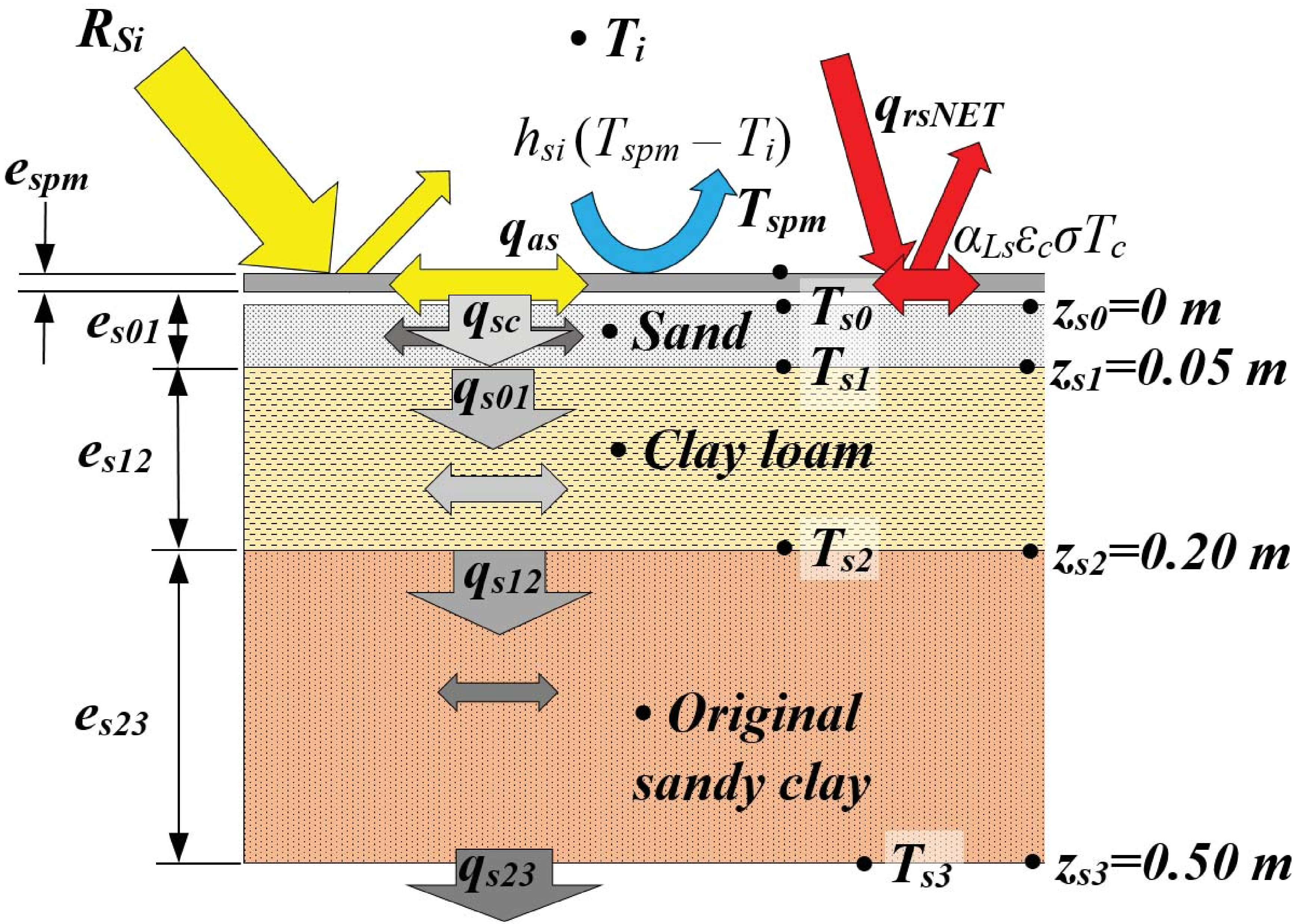

R_{Si}
T_i
$h_{si}(T_{spm} - T_i)$
q_{rsNET}
e_{spm}
q_{as}
T_{spm}
$\alpha_{Ls}\varepsilon_c\sigma T_c$
e_{s01}
q_{sc}
Sand
T_{s0}
z_{s0}=0 m
T_{s1}
z_{s1}=0.05 m
q_{s01}
e_{s12}
Clay loam
T_{s2}
z_{s2}=0.20 m
q_{s12}
e_{s23}
Original
sandy clay
T_{s3}
z_{s3}=0.50 m
q_{s23}

a)

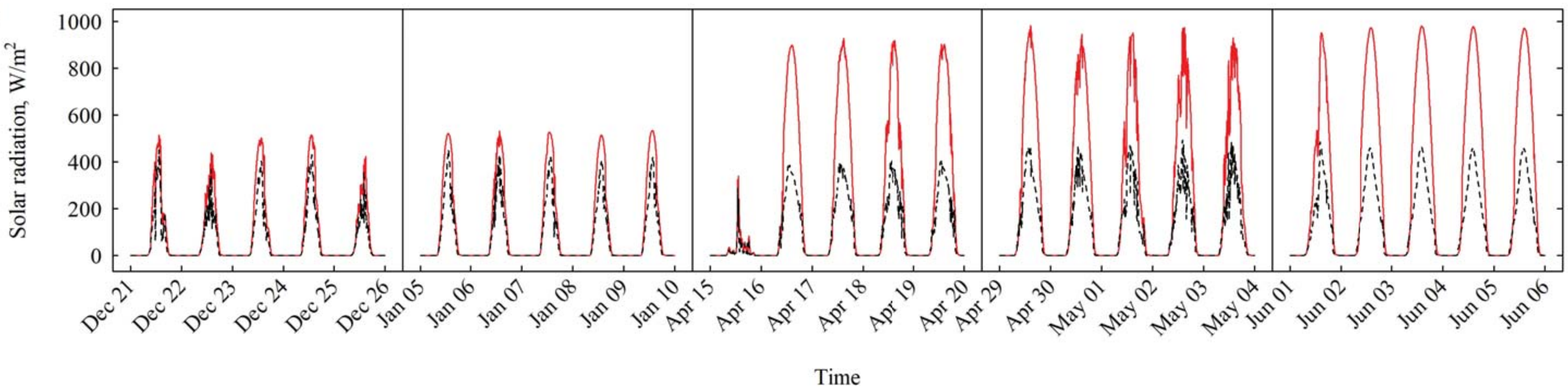
Solar radiation, W/m²
1000
800
600
400
200
0
Dec 21
Dec 22
Dec 23
Dec 24
Dec 25
Dec 26
Jan 05
Jan 06
Jan 07
Jan 08
Jan 09
Jan 10
Apr 15
Apr 16
Apr 17
Apr 18
Apr 19
Apr 20
Apr 29
Apr 30
May 01
May 02
May 03
May 04
Jun 01
Jun 02
Jun 03
Jun 04
Jun 05
Jun 06
Time

b)

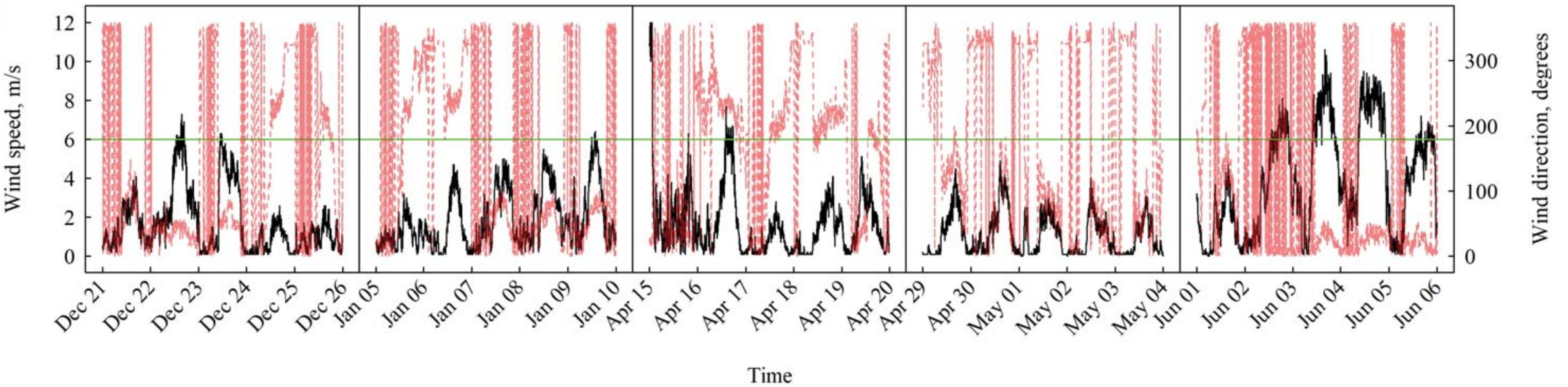

Wind speed, m/s
Wind direction, degrees
Time
Dec 21
Dec 22
Dec 23
Dec 24
Dec 25
Dec 26
Jan 05
Jan 06
Jan 07
Jan 08
Jan 09
Jan 10
Apr 15
Apr 16
Apr 17
Apr 18
Apr 19
Apr 20
Apr 29
Apr 30
May 01
May 02
May 03
May 04
Jun 01
Jun 02
Jun 03
Jun 04
Jun 05
Jun 06

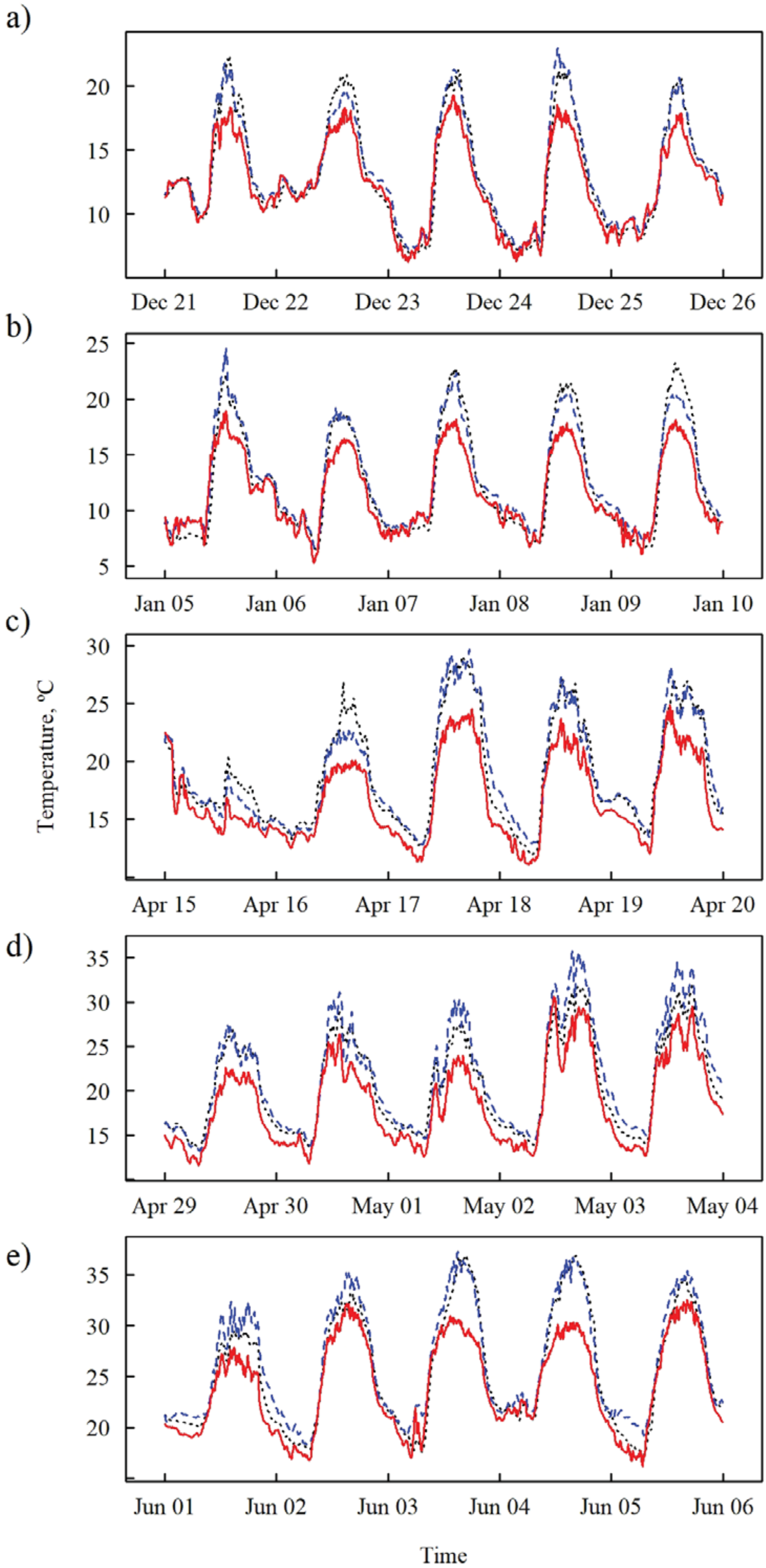
a)
b)
c)
d)
e)
Temperature, °C
Time
Dec 21
Dec 22
Dec 23
Dec 24
Dec 25
Dec 26
Jan 05
Jan 06
Jan 07
Jan 08
Jan 09
Jan 10
Apr 15
Apr 16
Apr 17
Apr 18
Apr 19
Apr 20
Apr 29
Apr 30
May 01
May 02
May 03
May 04
Jun 01
Jun 02
Jun 03
Jun 04
Jun 05
Jun 06

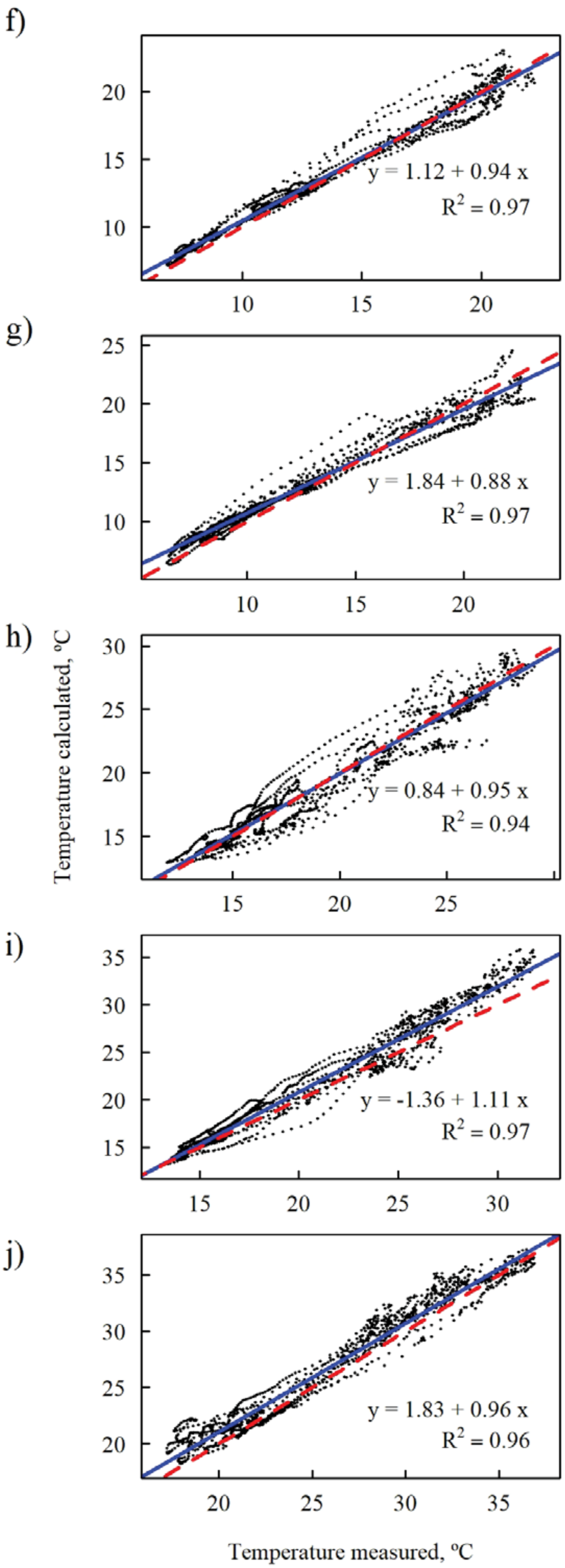

f)
y = 1.12 + 0.94 x
R2 = 0.97
g)
y = 1.84 + 0.88 x
R2 = 0.97
h)
y = 0.84 + 0.95 x
R2 = 0.94
i)
y = -1.36 + 1.11 x
R2 = 0.97
j)
y = 1.83 + 0.96 x
R2 = 0.96
Temperature calculated, ºC
Temperature measured, ºC

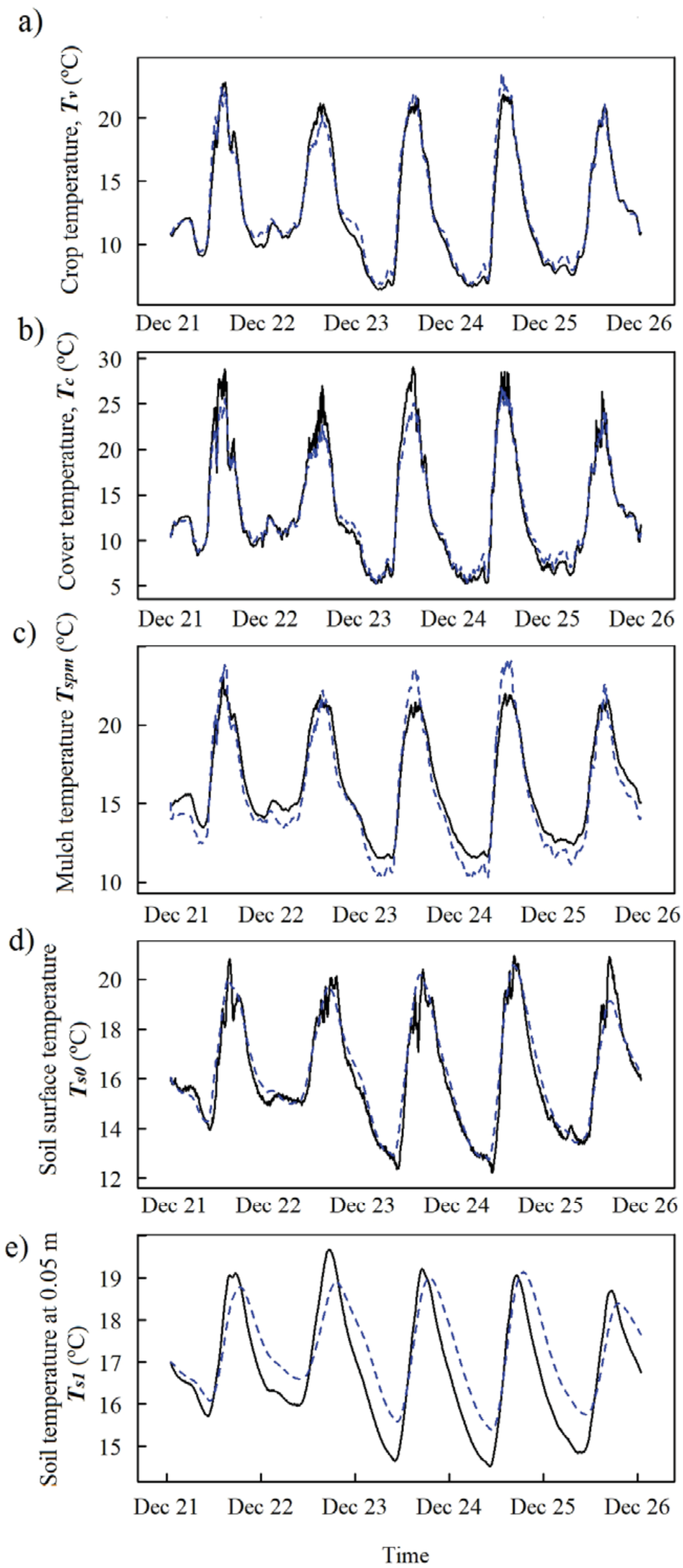
a)
Crop temperature, T_v (ºC)
10
15
20
Dec 21
Dec 22
Dec 23
Dec 24
Dec 25
Dec 26
b)
Cover temperature, T_c (ºC)
5
10
15
20
25
30
Dec 21
Dec 22
Dec 23
Dec 24
Dec 25
Dec 26
c)
Mulch temperature T_{spm} (ºC)
10
15
20
Dec 21
Dec 22
Dec 23
Dec 24
Dec 25
Dec 26
d)
Soil surface temperature T_{s0} (ºC)
12
14
16
18
20
Dec 21
Dec 22
Dec 23
Dec 24
Dec 25
Dec 26
e)
Soil temperature at 0.05 m T_{s1} (ºC)
15
16
17
18
19
Dec 21
Dec 22
Dec 23
Dec 24
Dec 25
Dec 26
Time

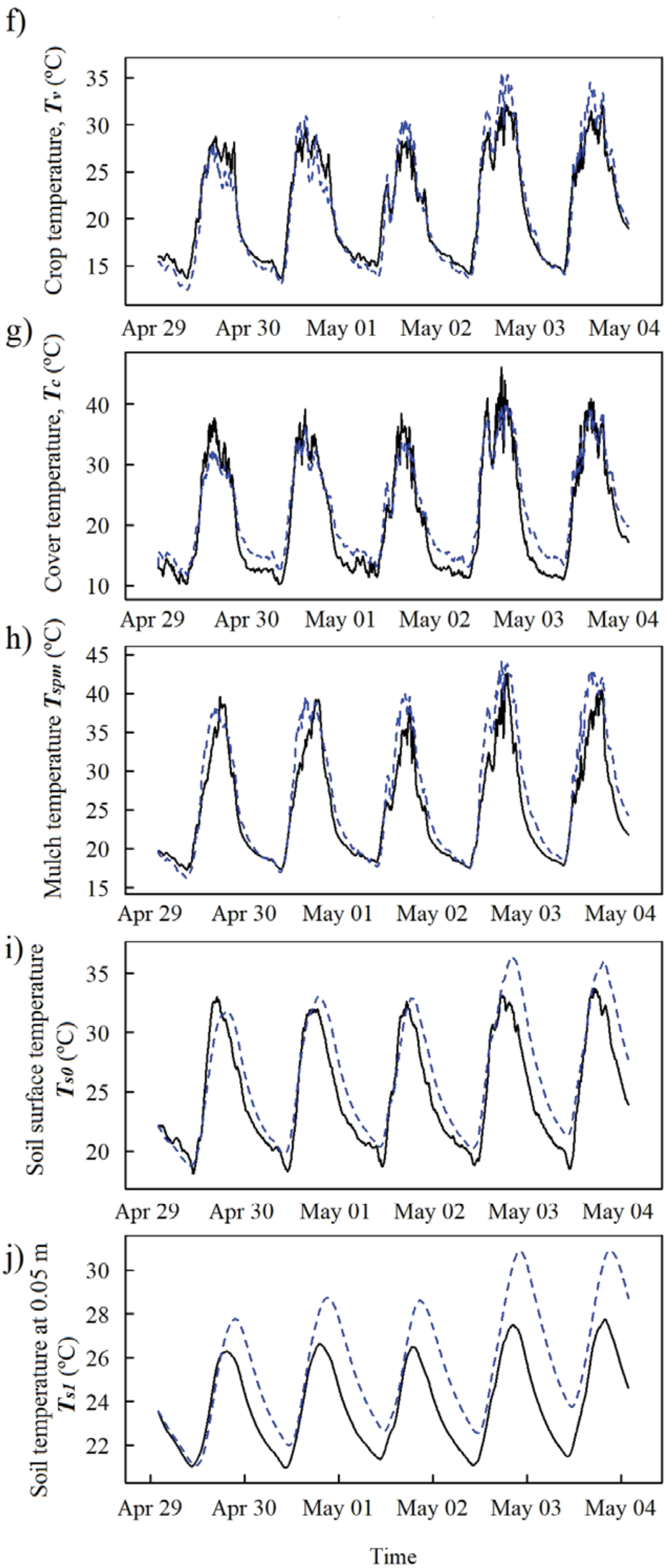
f)
Crop temperature, Tv (°C)
35
30
25
20
15
Apr 29
Apr 30
May 01
May 02
May 03
May 04
g)
Cover temperature, Tc (°C)
40
30
20
10
Apr 29
Apr 30
May 01
May 02
May 03
May 04
h)
Mulch temperature Tspm (°C)
45
40
35
30
25
20
15
Apr 29
Apr 30
May 01
May 02
May 03
May 04
i)
Soil surface temperature Ts0 (°C)
35
30
25
20
Apr 29
Apr 30
May 01
May 02
May 03
May 04
j)
Soil temperature at 0.05 m Ts1 (°C)
30
28
26
24
22
Apr 29
Apr 30
May 01
May 02
May 03
May 04
Time

a)

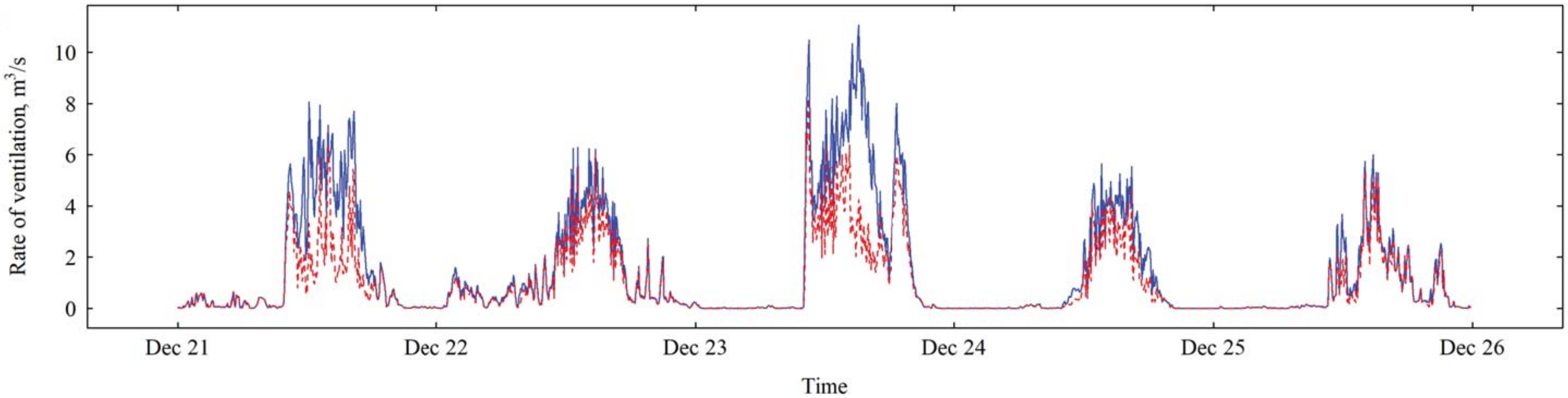

Rate of ventilation, m3/s
10
8
6
4
2
0
Dec 21
Dec 22
Dec 23
Dec 24
Dec 25
Dec 26
Time

b)

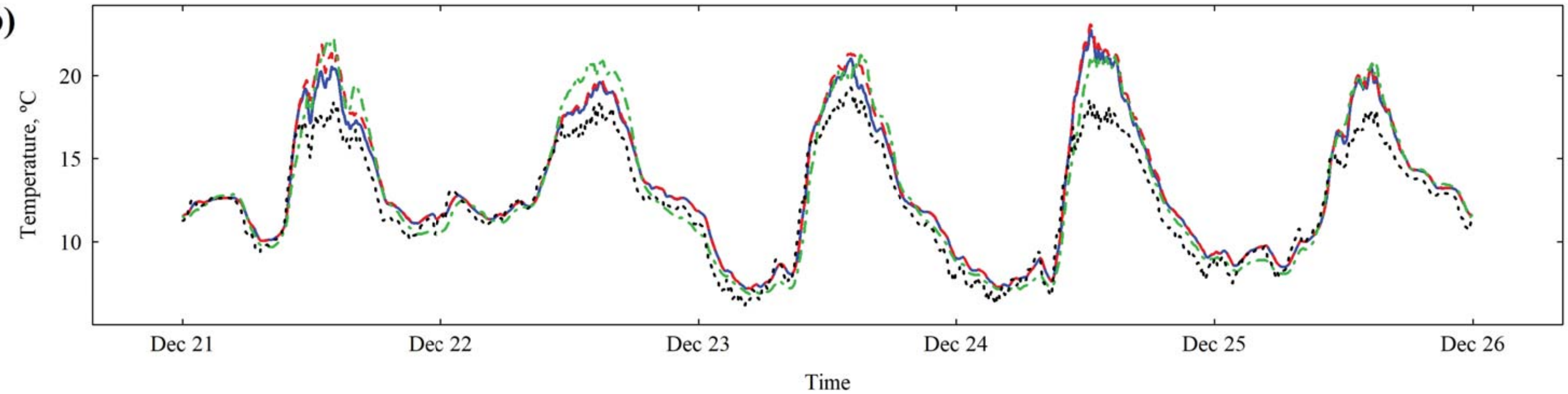

Temperature, °C
20
15
10
Dec 21
Dec 22
Dec 23
Dec 24
Dec 25
Dec 26
Time

a)

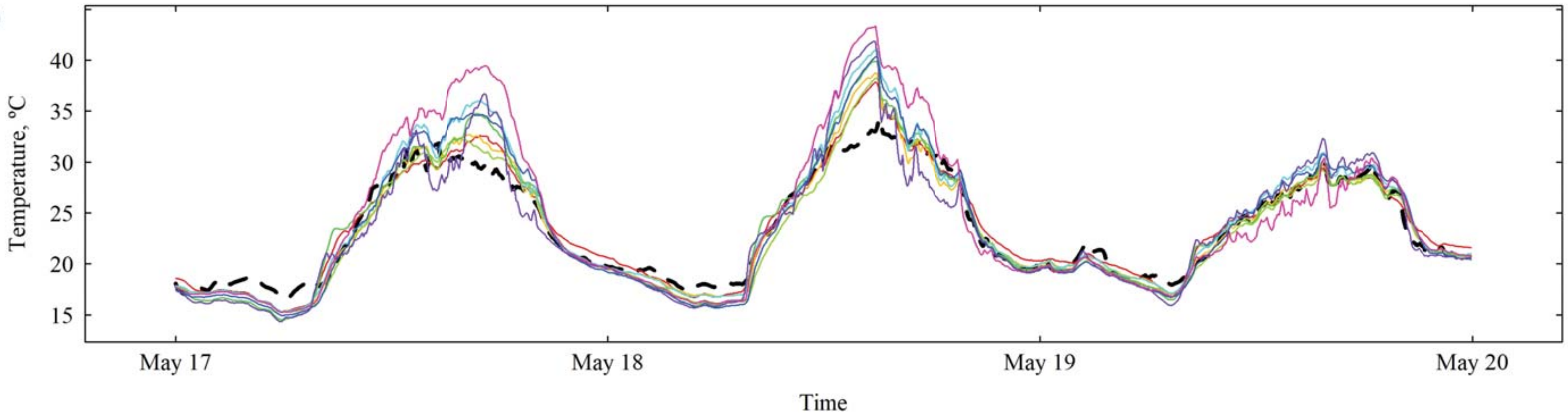

b)

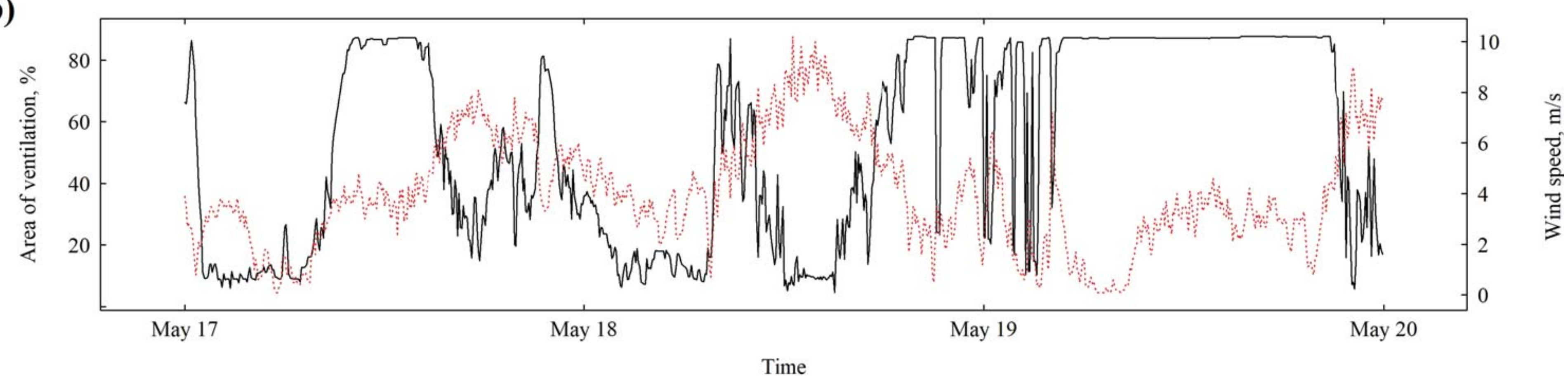

Area of ventilation, %
80
60
40
20
Wind speed, m/s
10
8
6
4
2
0
May 17
May 18
May 19
May 20
Time

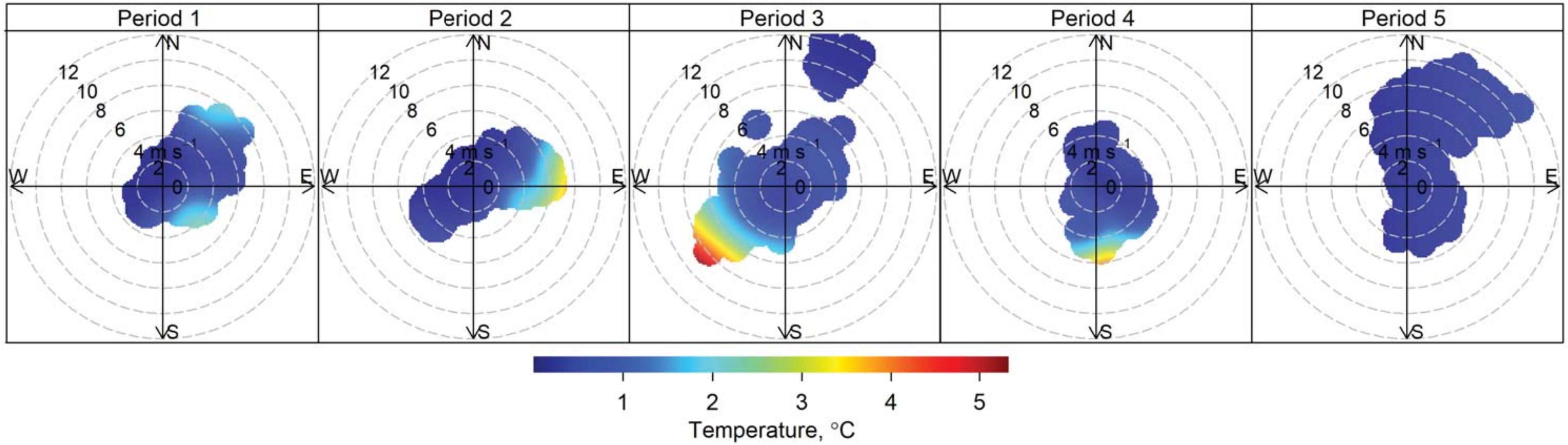

Period 1
Period 2
Period 3
Period 4
Period 5
N
E
S
W
12
10
8
6
4 m s -1
2
0
1
2
3
4
5
Temperature, °C

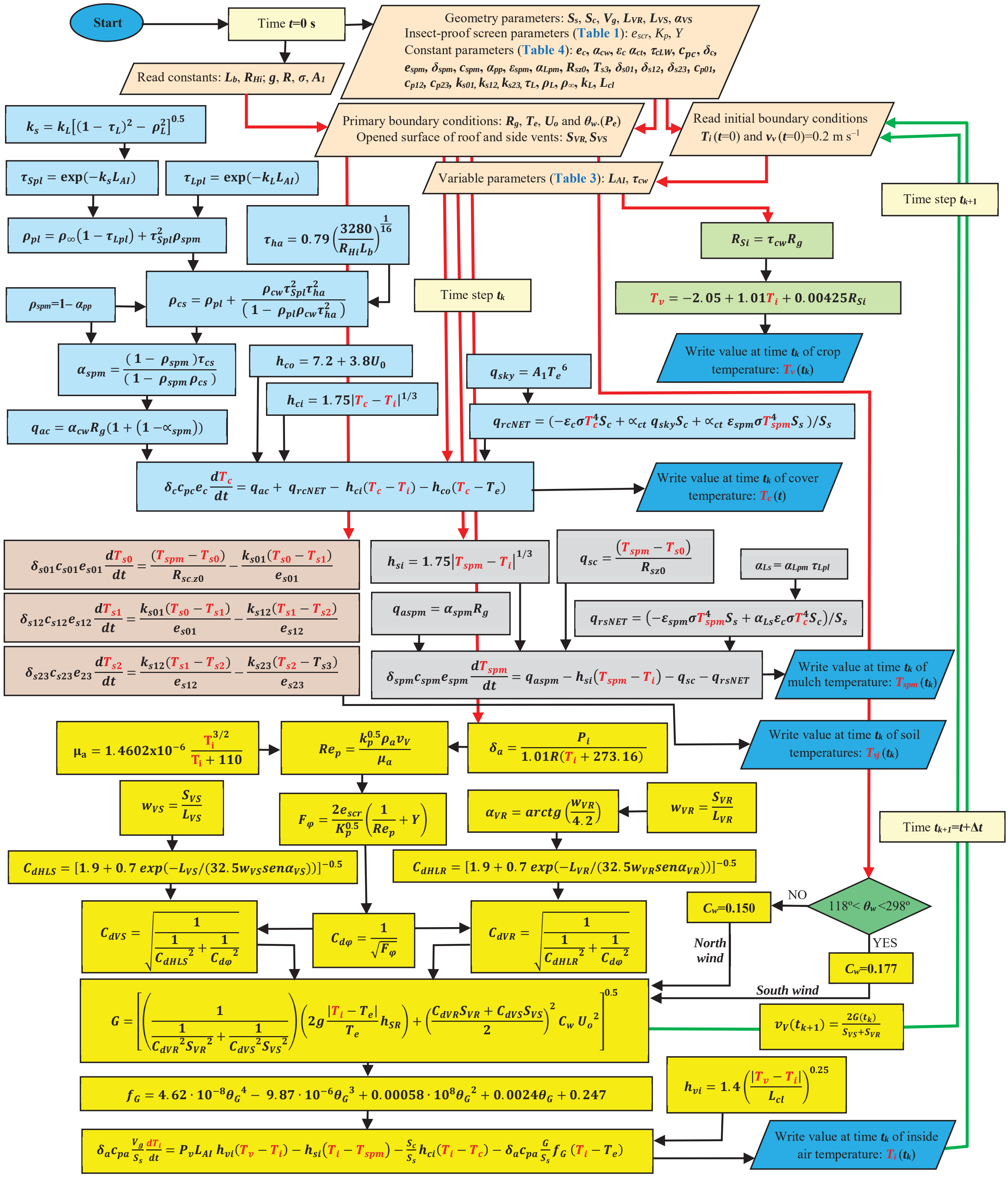

$$k_s = k_L[(1-\tau_L)^2 - \rho_L^2]^{0.5}$$

$$\tau_{Spl} = \exp(-k_s L_{AI}) \qquad \tau_{Lpl} = \exp(-k_L L_{AI})$$

$$\rho_{pl} = \rho_\infty(1-\tau_{Lpl}) + \tau_{Spl}^2\rho_{spm}$$

$$\tau_{ha} = 0.79\left(\frac{3280}{R_{Hi}L_b}\right)^{\frac{1}{16}}$$

$$\rho_{spm} = 1 - \alpha_{pp}$$

$$\rho_{cs} = \rho_{pl} + \frac{\rho_{cw}\tau_{Spl}^2\tau_{ha}^2}{(1-\rho_{pl}\rho_{cw}\tau_{ha}^2)}$$

$$\alpha_{spm} = \frac{(1-\rho_{spm})\tau_{cs}}{(1-\rho_{spm}\rho_{cs})}$$

$$h_{co} = 7.2 + 3.8U_0$$

$$h_{ci} = 1.75|T_c - T_i|^{1/3}$$

$$q_{sky} = A_1 T_e^{\,6}$$

$$R_{Si} = \tau_{cw}R_g$$

$$T_v = -2.05 + 1.01T_i + 0.00425R_{Si}$$

$$q_{ac} = \alpha_{cw}R_g(1 + (1 - \alpha_{spm}))$$

$$q_{rcNET} = (-\varepsilon_c\sigma T_c^4 S_c + \alpha_{ct}\, q_{sky}S_c + \alpha_{ct}\,\varepsilon_{spm}\sigma T_{spm}^4 S_s)/S_s$$

$$\delta_c c_{pc} e_c \frac{dT_c}{dt} = q_{ac} + q_{rcNET} - h_{ci}(T_c - T_i) - h_{co}(T_c - T_e)$$

$$\delta_{s01}c_{s01}e_{s01}\frac{dT_{s0}}{dt} = \frac{(T_{spm}-T_{s0})}{R_{sc.z0}} - \frac{k_{s01}(T_{s0}-T_{s1})}{e_{s01}}$$

$$\delta_{s12}c_{s12}e_{s12}\frac{dT_{s1}}{dt} = \frac{k_{s01}(T_{s0}-T_{s1})}{e_{s01}} - \frac{k_{s12}(T_{s1}-T_{s2})}{e_{s12}}$$

$$\delta_{s23}c_{s23}e_{23}\frac{dT_{s2}}{dt} = \frac{k_{s12}(T_{s1}-T_{s2})}{e_{s12}} - \frac{k_{s23}(T_{s2}-T_{s3})}{e_{s23}}$$

$$h_{si} = 1.75|T_{spm} - T_i|^{1/3}$$

$$q_{sc} = \frac{(T_{spm}-T_{s0})}{R_{sz0}}$$

$$\alpha_{Ls} = \alpha_{Lpm}\,\tau_{Lpl}$$

$$q_{aspm} = \alpha_{spm}R_g$$

$$q_{rsNET} = (-\varepsilon_{spm}\sigma T_{spm}^4 S_s + \alpha_{Ls}\varepsilon_c\sigma T_c^4 S_c)/S_s$$

$$\delta_{spm}c_{spm}e_{spm}\frac{dT_{spm}}{dt} = q_{aspm} - h_{si}(T_{spm} - T_i) - q_{sc} - q_{rsNET}$$

$$\mu_a = 1.4602\text{x}10^{-6}\frac{T_i^{3/2}}{T_i + 110}$$

$$Re_p = \frac{k_p^{0.5}\rho_a v_V}{\mu_a}$$

$$\delta_a = \frac{P_i}{1.01R(T_i + 273.16)}$$

$$w_{VS} = \frac{S_{VS}}{L_{VS}}$$

$$F_\varphi = \frac{2e_{scr}}{K_p^{0.5}}\left(\frac{1}{Re_p} + Y\right)$$

$$\alpha_{VR} = arctg\left(\frac{w_{VR}}{4.2}\right)$$

$$w_{VR} = \frac{S_{VR}}{L_{VR}}$$

$$C_{dHLS} = [1.9 + 0.7\,exp(-L_{VS}/(32.5w_{VS}sen\alpha_{VS}))]^{-0.5}$$

$$C_{dHLR} = [1.9 + 0.7\,exp(-L_{VR}/(32.5w_{VR}sen\alpha_{VR}))]^{-0.5}$$

$$118^{o} < \theta_w < 298^{o}$$

$$C_{dVS} = \sqrt{\frac{1}{\frac{1}{C_{dHLS}^{\;2}} + \frac{1}{C_{d\varphi}^{\;2}}}}$$

$$C_{d\varphi} = \frac{1}{\sqrt{F_\varphi}}$$

$$C_{dVR} = \sqrt{\frac{1}{\frac{1}{C_{dHLR}^{\;2}} + \frac{1}{C_{d\varphi}^{\;2}}}}$$

$$G = \left[\left(\frac{1}{\frac{1}{C_{dVR}^{\;2}S_{VR}^{\;2}} + \frac{1}{C_{dVS}^{\;2}S_{VS}^{\;2}}}\right)\left(2g\frac{|T_i - T_e|}{T_e}h_{SR}\right) + \left(\frac{C_{dVR}S_{VR} + C_{dVS}S_{VS}}{2}\right)^2 C_w\,U_o^{\;2}\right]^{0.5}$$

$$v_V(t_{k+1}) = \frac{2G(t_k)}{S_{VS}+S_{VR}}$$

$$f_G = 4.62\cdot10^{-8}\theta_G^{\;4} - 9.87\cdot10^{-6}\theta_G^{\;3} + 0.00058\cdot10^{8}\theta_G^{\;2} + 0.0024\theta_G + 0.247$$

$$h_{vi} = 1.4\left(\frac{|T_v - T_i|}{L_{cl}}\right)^{0.25}$$

$$\delta_a c_{pa}\frac{V_g}{S_s}\frac{dT_i}{dt} = P_v L_{AI}\,h_{vi}(T_v - T_i) - h_{si}(T_i - T_{spm}) - \frac{S_c}{S_s}h_{ci}(T_i - T_c) - \delta_a c_{pa}\frac{G}{S_s}f_G\,(T_i - T_e)$$